

**A STUDY OF THE
TRANSIENT CORRECTION FACTOR USED IN
TREAT REACTOR IN-PILE EXPERIMENTS**

by

Dale L. Graff

BASE TECHNOLOGY



U of C - ANL - USDOE

ARGONNE NATIONAL LABORATORY, ARGONNE, ILLINOIS

**Prepared for the U. S. DEPARTMENT OF ENERGY
under Contract W-31-109-Eng-38**

The facilities of Argonne National Laboratory are owned by the United States Government. Under the terms of a contract (W-31-109-Eng-38) between the U. S. Department of Energy, Argonne Universities Association and The University of Chicago, the University employs the staff and operates the Laboratory in accordance with policies and programs formulated, approved and reviewed by the Association.

MEMBERS OF ARGONNE UNIVERSITIES ASSOCIATION

The University of Arizona	Kansas State University	The Ohio State University
Carnegie-Mellon University	The University of Kansas	Ohio University
Case Western Reserve University	Loyola University	The Pennsylvania State University
The University of Chicago	Marquette University	Purdue University
University of Cincinnati	Michigan State University	Saint Louis University
Illinois Institute of Technology	The University of Michigan	Southern Illinois University
University of Illinois	University of Minnesota	The University of Texas at Austin
Indiana University	University of Missouri	Washington University
Iowa State University	Northwestern University	Wayne State University
The University of Iowa	University of Notre Dame	The University of Wisconsin

NOTICE

This report was prepared as an account of work sponsored by the United States Government. Neither the United States nor the United States Department of Energy, nor any of their employees, nor any of their contractors, subcontractors, or their employees, makes any warranty, express or implied, or assumes any legal liability or responsibility for the accuracy, completeness or usefulness of any information, apparatus, product or process disclosed, or represents that its use would not infringe privately-owned rights. Mention of commercial products, their manufacturers, or their suppliers in this publication does not imply or connote approval or disapproval of the product by Argonne National Laboratory or the U. S. Department of Energy.

Printed in the United States of America
Available from
National Technical Information Service
U. S. Department of Commerce
5285 Port Royal Road
Springfield, Virginia 22161
Price: Printed Copy \$5.25; Microfiche \$3.00

ANL-78-31

ARGONNE NATIONAL LABORATORY
9700 South Cass Avenue
Argonne, Illinois 60439

A STUDY OF THE
TRANSIENT CORRECTION FACTOR USED IN
TREAT REACTOR IN-PILE EXPERIMENTS

by

Dale L. Graff

Reactor Analysis and Safety Division

March 1978

Based on a thesis submitted to
the Graduate School of
Purdue University
in partial fulfillment of the requirements
for the degree of
Master of Science
in the field of Nuclear Engineering

TABLE OF CONTENTS

	<u>Page</u>
ABSTRACT	7
I. INTRODUCTION	8
Background	8
Statement of the Problem	9
The Scope and Organization of the Thesis	9
II. THE TREAT REACTOR AND THE F-1 AND EOS-1 EXPERIMENTS	11
F-1 and EOS-1 Experiments	11
The TREAT Reactor	11
The F-1 Test	12
The EOS-1 Test	14
III. POWER CALIBRATION TESTS FOR F-1 AND EOS-1	18
Alternatives to the TCF Method	18
Control-rod Shadowing of TREAT Instrumentation	18
Results of F-1 Calibration Test	21
Results of the EOS-1 Calibration Test	22
IV. COMPUTER MODELING OF THE CALIBRATION TESTS	25
General Approach	25
Cross Sections	25
Reactor Modeling Using the ANISN Code	26
V. RESULTS	29
Interpreting ANISN Output	29
Computed F-1 Transient Correction Factors	29
Computed EOS-1 Transient Correction Factors	31
Transient Correction Factors for Clipped and F-2 Transients	34

TABLE OF CONTENTS

	<u>Page</u>
VI. SUMMARY AND CONCLUSIONS	36
Summary	36
Conclusions	36
APPENDICES	39
A. A Description of the TREAT Reactor	39
B. Descriptions of the F-1 and EOS-1 Fuel Pins and Zr-U Monitor Wires	45
C. The AMPX Systems and Neutron-cross- section Data Set Generation	48
D. The Discrete-ordinates Method and the ANISN Code	51
E. Boron Cross Sections for Control Rods	53
ACKNOWLEDGMENTS	55
REFERENCES	56

LIST OF FIGURES

<u>No.</u>	<u>Title</u>	<u>Page</u>
1	Cutaway View of the TREAT Reactor	11
2	Modified Mark-II Loop	12
3	Cutaway View of the F-1 Test Capsule	13
4	Radial Cross Section of the F-1 Pressure Vessel	15
5	Core-loading Map for F-1 Test	15
6	Cutaway View of the EOS-1 Test Capsule	17
7	ANISN Representation of TREAT Core	26
A-1	Standard TREAT Fuel Assembly	40
A-2	Types of TREAT Fuel Assemblies	41
C-1	Possible Paths between the Major AMPX Modules	49

LIST OF TABLES

<u>No.</u>	<u>Title</u>	<u>Page</u>
1	Alternatives to Determine Calibration Factors	19
2	TREAT Instrument Calibrations for Two Steady State Runs	20
3	Summary of Transients for the F-Series Calibration Test	23
4	Summary of Selected EOS-1 Calibration Test Transients	24
5	Results of F-1 ANISN Runs	30
6	Results of EOS-1 ANISN Runs	32
7	Results of Modified F-1 ANISN Runs	33
8	ANISN Results for Clipped and F-2 Transients	34
A-1	Material Composition of TREAT Fuel	39
B-1	F-1 Fuel Pin Data	45
B-2	EOS-1 Upper Test Pin Description	46

LIST OF TABLES

<u>No.</u>	<u>Title</u>	<u>Page</u>
B-3	EOS-1 Lower Control Pin Description	47
B-4	Description of Zr-U Monitor Wires	47
E-1	Changes to Boron Capture Cross Sections by Group	54

A STUDY OF THE TRANSIENT CORRECTION FACTOR USED
IN TREAT REACTOR IN-PILE EXPERIMENTS

by

Dale L. Graff

ABSTRACT

The transient correction factor (TCF) is used in TREAT reactor experiments to predict the power calibration coefficient (PC) for prototype LMFBR fuel pins at transient conditions without subjecting the pins to a reactor transient. The TCF is defined as the fissions in a monitor wire per MW of reactor power at transient conditions divided by the fissions in a monitor wire per MW of reactor power at low power conditions. The power calibration factor is the power in the target fuel per gram of ^{235}U per MW reactor power.

The purpose of this study was to reduce the uncertainties concerning the transient correction factor by examining the nature and applicability of the TCF method.

ANISN, a discrete-ordinates transport code, was used to simulate two TREAT reactor tests. The computer results showed that the relative positions of the TREAT control rods for low-level and transient power runs are the major cause of the transient correction factor. A secondary determining factor is the heating of the steel structure surrounding the target.

It was concluded that for the single-pin experiments, the monitor-wire transient correction factor method will produce reasonably accurate predictions of the fuel-pin power calibration coefficients.

I. INTRODUCTION

Background

The TREAT reactor is a large, graphite-moderated research reactor operated by Argonne National Laboratory and located at the National Reactor Testing Station in Idaho. It is currently used to irradiate prototype fast-reactor fuel pins under conditions approximating fuel-failure accidents. The purpose of the experiments is to improve LMFBR design concepts by studying the mechanics of fuel-pin failure and postfailure events.

The experiments are conducted by lowering a stainless steel pressure vessel containing the target prototype pins into a hole in the center of the reactor. The vessel is usually loop-shaped and fitted with a linear induction pump that provides the pins with the liquid-sodium cooling. Accidents involving loss of coolant flow (LOF) to the pins are simulated by programming the pump to terminate the flow.

The experiments are also designed to simulate transient-overpower (TOP) accidents. Computer-aided control of the reactor provides the necessary neutronics environment. The TREAT thermal-neutron spectrum is hardened by surrounding the pressure vessel with thermal-neutron filters of boron and/or dysprosium. The power transients of the TREAT reactor combined with the coolant effects of the loop lead to the destruction of the target pins.

During the experiments, thermocouples and pressure transducers monitor the thermal environment in the vessel. Neutron detectors positioned outside the core measure the reactor power. However, the power produced in the pins, an essential parameter of the experiments, is not measured directly. Instead, it is determined following the test by multiplying the measured reactor power by a power calibration factor. This factor relates the power in the target pins to the TREAT reactor power.

The power calibration factor must be known prior to the experiment for planning the appropriate transient. Only for experiments with similar power transients and target pin configurations can the same calibration factor be used. An iterative procedure for determining the power calibration factor and for choosing the proper reactor transient is not feasible because of the limited numbers of pins.

A method was devised to predict the calibration factor without subjecting target fuel pins to transient conditions. In this method, a power calibration factor is determined for target pins irradiated at low-level steady-state power in the reactor. The calibration is then modified to transient power by using a transient correction factor (TCF).

The TCF is calculated in the following manner:

1. The fuel pins in the vessel are replaced by monitor wires which contain a very much lower concentration of fissile material. The wires are irradiated at the same low-level steady-state power as the fuel pins. Following the irradiation, the monitor wires are analyzed for the number of fissions.

2. A new set of monitor wires are placed in the vessel and irradiated with a reactor transient. After the test, the fissions that occurred in the wires are counted.
3. The ratio of the monitor-wire fissions at transient power to the monitor-wire fissions at low power is calculated. The ratio, called the transient correction factor, is multiplied by the power calibration factor for the fuel pins at low power to predict the fuel-pin power calibration factor for the transient.

Statement of the Problem

The transient correction factor has produced adequate predictions of the power calibration factor in previous experiments. However, it is not generally known why this occurs. The assumption that the monitor wires act the same as the fuel pins in going from low to transient power conditions is difficult to prove. First, the monitor wires, containing 93% ^{235}U in uranium, replace fuel pins that in the experiments range from natural to full enrichment. The monitor-wire temperatures are not the same as the fuel pins during transient conditions. Moreover, the size of the monitor wires prevents the neutron shadowing that normally occurs in a cluster of fuel pins.

Another problem is that the transient correction factor is in itself difficult to predict. Situations have occurred in which computer calculations and previous experience have pointed to a particular value for the TCF which was totally different than the experimental value.

Finally, experimenters are not sure why a correction factor is needed (i.e., why the TCF is not equal to 1.0?).

The Scope and Organization of the Thesis

This study will concentrate on explaining the transient correction factor - its origin and usefulness in predicting the power calibration factor. The data for the study are taken from the tests used to determine the transient correction factors and power calibration factors for two experiments, the F-1 and EOS-1 experiments.* Computer calculations using reactor-physics codes serve as the primary research tool by simulating the various tests.

The F-1 and the EOS-1 experiments were selected for certain advantageous reasons. The geometry is simple; both tests did not involve fuel-pin clusters. The F-1 test had a single pin, while the EOS-1 test had two fuel pins arranged along the same axis but separated from each other in the pressure vessel. The linear induction pump was removed for both experiments, which also simplified the geometry and prevented shadowing of the fuel pins by the pump. Because these tests were the first experiments in their respective series, calibration of the fuel pins received special attention, and many different tests were performed to determine the proper factors. Finally, despite their apparent similarities, the tests produced very different transient correction factors.

* These tests are discussed in detail in Chapter 2.

The following chapters will describe in more detail the F-1 and EOS-1 experiments and their correction factors, as well as the TREAT reactor. Steps taken to simulate the experiments with the computer programs will also be described. Following this, there will be an analysis of the computer results and a discussion of the conclusions of the study.

II. THE TREAT REACTOR AND THE F-1 AND EOS-1 EXPERIMENTS

The TREAT Reactor¹

The Transient Reactor Test facility (TREAT) is illustrated in Fig. 1 and briefly described below. A more complete discussion of the reactor is included as Appendix A.

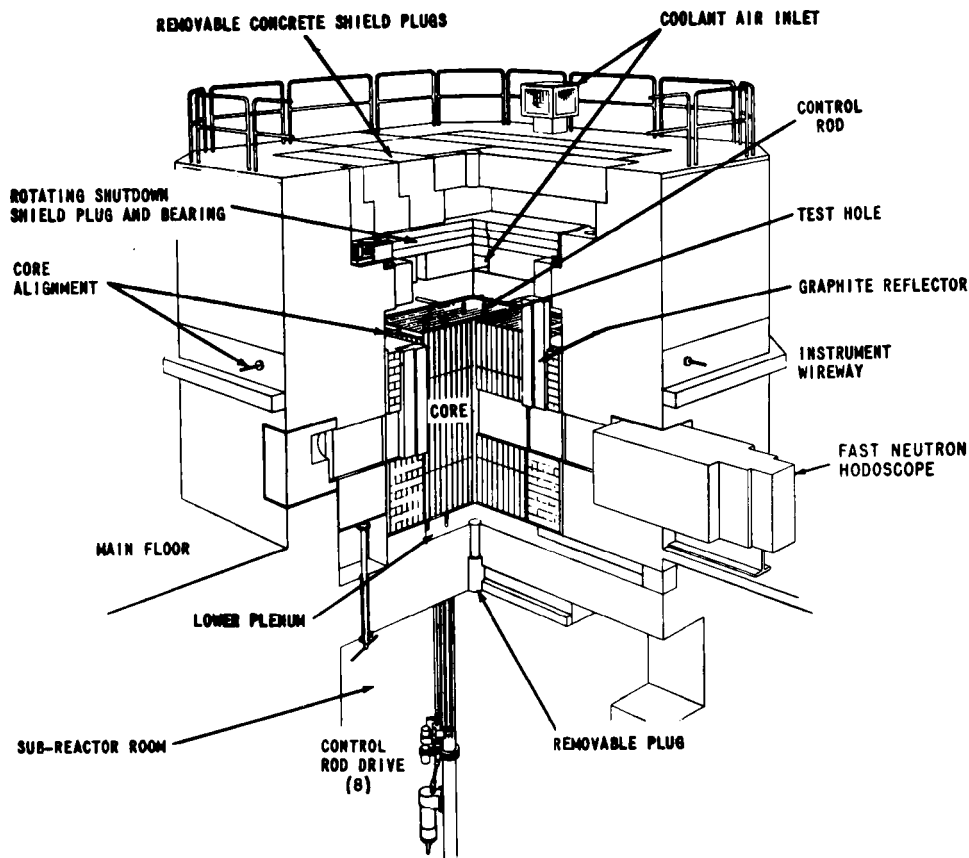


Fig. 1. Cutaway View of the TREAT Reactor
(ANL Neg. No. 900-2776).

The active core region of TREAT, commonly referred to as the driver, consists of fully enriched uranium mixed in graphite. The ratio of carbon atoms to uranium atoms is about 10,000 to 1. The standard fuel assemblies measure 10.05 cm (3.96 in.) on a side and have an active fuel height of 1.2 m (4 ft.). In addition to these, there are control-rod, dummy, and slotted-fuel assemblies. The latter have 55.245 by 8.89 cm (21.75 by 3.5 in.) slots through them which are used for access to the fission neutrons generated in the target fuel. The core holds 361 assemblies in a 19x19 array.

Control of the reactor is maintained by 9 pairs of boron carbide control rods arranged to form two rings about the core center. During a typical transient, one pair of rods from each ring shape the reactor power, while the others are used for reactor shutdown. Two types of transients are possible in TREAT: peaked bursts and shaped bursts. The first is generated by an initial

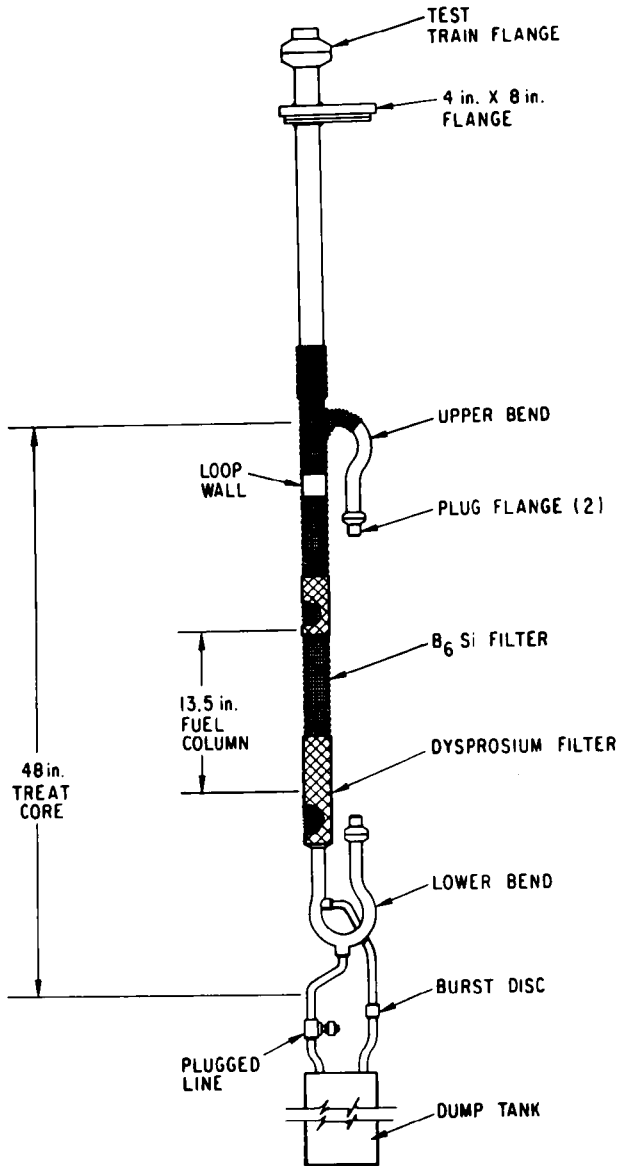


Fig. 2. Modified Mark-II Loop
(ANL Neg. No. 900-2269).

insertion of reactivity followed by a shutdown induced by the negative temperature coefficient of the reactor. Shaped transients result from combining power flat-tops (where the power is held constant after an initial rise) with power bursts (where the reactor period is constant). Information on reactor power and period comes from boron-10-coated ion chambers surrounding the outside of the core.

The F-1 Test

The purpose of the TREAT F-series of experiments is "...to provide data on fuel motion at accident power levels from one to about ten times design, for use in development of the fuel motion models."² The first experiment in the F-series, F-1, was performed with moderate-burnup fuel in order to evaluate the effect of fission-gas release on molten-fuel dispersion. The type of accident simulated by the test was a hypothetical unprotected loss-of-flow accident in the Fast Flux Test Facility (FFTF).

A modified Mark-II loop, illustrated in Fig. 2, was used to hold the F-1 test pin capsule.³ The major change to the loop for the test was the removal of the linear induction

pump between the upper and lower bends. The pump was not needed, as the target pin was dry-sealed in the test capsule. Filtering of thermal neutrons in the F-1 test was accomplished with an 0.46-mm (18-mil)-thick layer of B_6Si painted on a wire mesh around the outside of the loop. The reason for the hardening of the TREAT spectrum in this manner was to ensure the desired progression of melting in the target pin prior to fuel motion. Collars of dysprosium were added over the layer of B_6Si near the ends of the target pin to act as thermal-neutron filters to shape the axial flux. In this manner the neutron flux densities were made to conform as nearly as possible to the relative axial burnup shape resulting from irradiation in EBR-II.

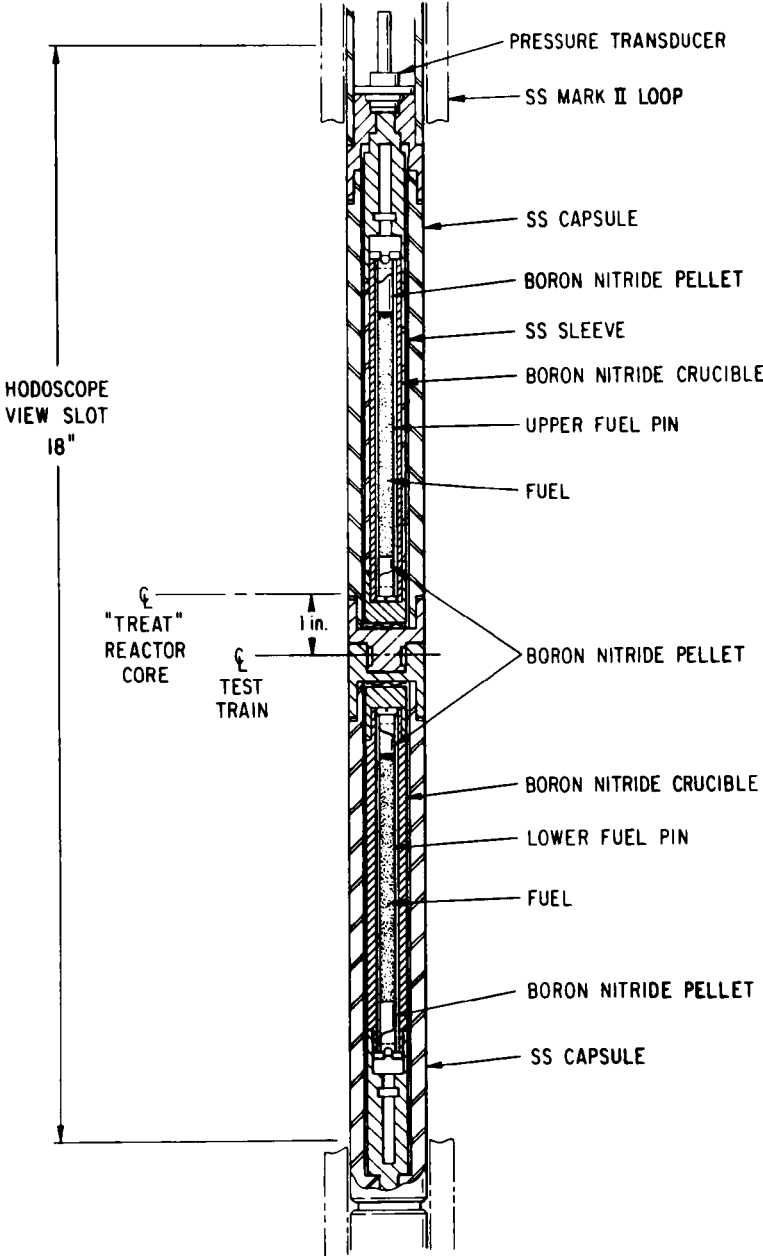


Fig. 3. Cutaway View of the F-1 Test Capsule (ANL Neg. No. 900-5270 Rev. 2).

The F-1 test capsule, which is shown in Fig. 3, contained the target fuel pin, a nuclear-heated wall, a molybdenum reflector, and a stainless steel heat sink. The target pin was a mixture of 25% PuO₂ and 75% of UO₂, with the uranium enriched to 77% ²³⁵U. It was held in place at the bottom by a tungsten pin. The upper end was held by a retainer clip which permitted only upward movement of the target pin. More detail on the fuel pin is contained in Appendix B.

Figure 4 shows the radial cross section of the loop and test capsule at the fuel-pin centerline. All of the measurements in this diagram are expressed in inches (1 in. = 2.54 cm). The purpose of the nuclear-heated wall which is shown surrounding the fuel pin was to provide the pin with a thermal environment similar to accident conditions and a radial boundary for fuel motion.

The loop section containing the F-1 fuel pin was approximately centered in a TREAT core loading of 268 standard assemblies, 16 control-rod assemblies, 8 slotted assemblies, 1 dummy assembly, and 66 reflector assemblies (see Fig. 5). The eight slotted elements were arranged to form a viewing slot for the fast-neutron hodoscope* located at the northern face of the reactor. The eight pairs of control rods formed two rings: an inner ring with a radius of 46 cm, and an outer ring at 74 cm.

The core-loading map indicates the positions of the TREAT power instruments. The linear power instrument is located in the south side of the core about 6 assemblies west of core center. A steady-state period meter and a steady-state safety detector (not shown) are also located in this same position. Another set of period and safety detectors for use in steady-state operation are located on the west face of the core about 4 assemblies north of center. Detectors for determining reactor power, period, and integrated power during transients are located at the NW, SW, and SE corners of the core.

The control-rod pairs for the F-1 test were numbered as illustrated in the core-loading map. Control-rod pairs 2 and 9 were transient control rods which used high-speed hydraulic drives. For the computer-controlled F-1 transient, The T-2 rods (pair no. 9) were held at a constant position, while the T-1 rods (pair no. 2) were pulled to produce a flat-top power shape. All other rods were withdrawn from the core. The transient started with 200- μ s period, rising from zero power to about 70 MW in 4 s. This power level was held steady for 10 s and was followed by a SCRAM.

The EOS-1 Test

The first experiment in the Equation-of-State (EOS) test series was to provide data on the nature and timing of gas-driven disassembly from fuel-pin fission gas. The test employed two fuel pins that were sealed in separate stainless steel capsules and placed one above the other axially to form the test train.⁴

The upper fuel pin in the EOS series was designed to fail in order to supply fuel-motion data. For EOS-1, this test pin had fresh fuel that was

* See Appendix A.

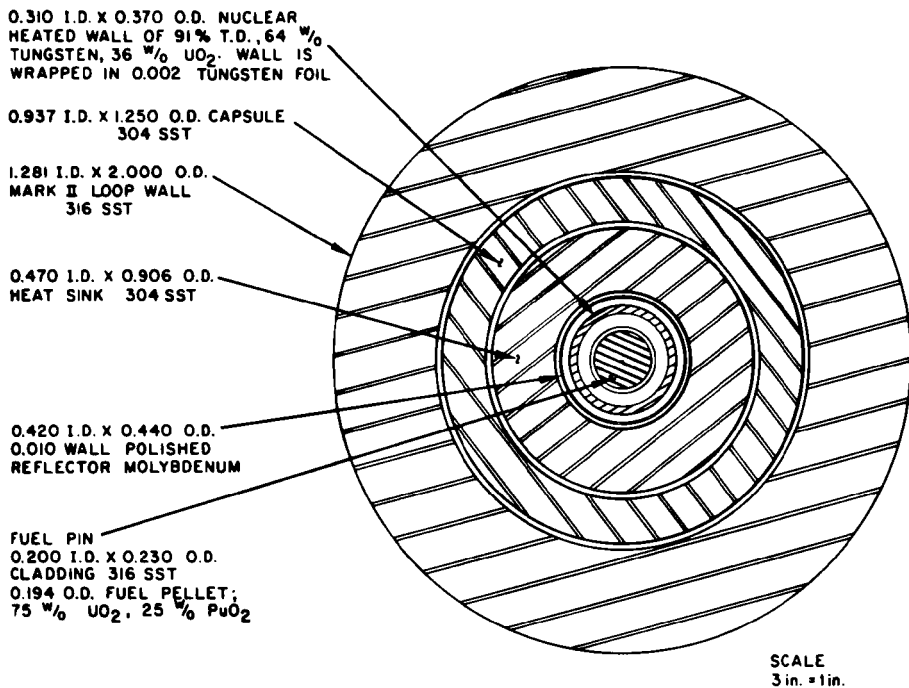


Fig. 4.

Radial Cross Section of the F-1 Pressure Vessel (ANL Neg. No. 900-5271).

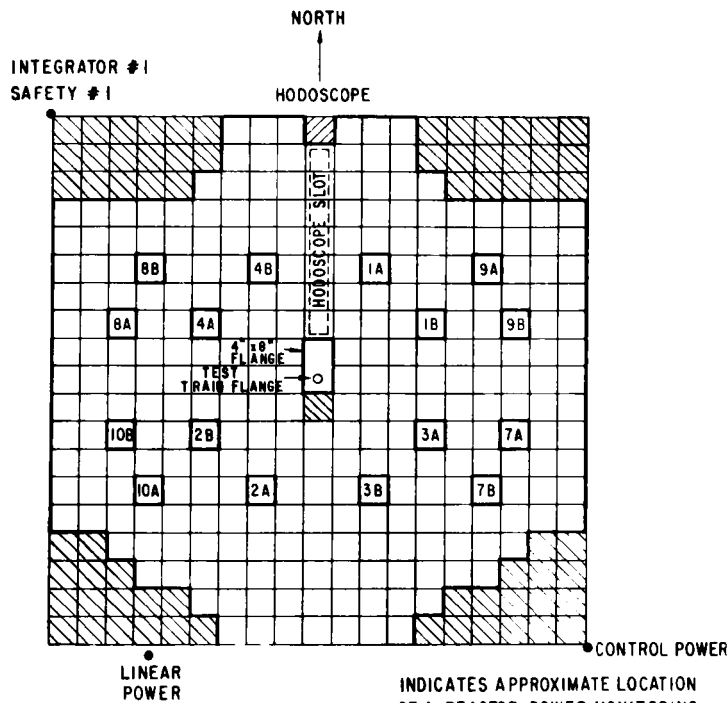


Fig. 5.

Core-loading Map for F-1 Test (ANL Neg. No. 900-75-61).

NOTE: CONTROL RODS ARE MOVED IN PAIRS (eg. 2A+2B) ONLY ROD PAIR 2A+2B REFERRED TO AS T-1 AND ROD PAIR 9A+9B REFERRED TO AS T-2 MAY BE MOVED DURING TRANSIENTS

enriched to 65% ^{235}U in uranium. The length of the fuel in the upper pin is 10 cm (4 in.) (see Fig. 6). The fuel in the pin was capped at both ends by boron nitride (BN) pellets with lengths of 13 cm (0.5 in.). Surrounding the upper pin was a 203-mm (90-mil)-thick BN containment can which acts both as a thermal-neutron filter and a ceramic crucible. A 2.3-mm (90-mil)-thick stainless steel sleeve having an outer diameter of 1.65 cm (0.65 in.) encloses the crucible.

The lower fuel pin was designed to maintain its geometry throughout the tests. The purpose of the pin was to supply fission neutrons for renormalization of the hodoscope data at the high power level of the test fuel. The uranium in the lower pin was not enriched. BN pellets capped the ends of the 10.2-cm (4-in.) section of the active fuel. The BN lower-pin crucible had a 1.65-cm (0.65 in.) outer diameter and was twice as thick as the upper crucible. (More information concerning the EOS-1 fuel pins is available in Appendix B).

The crucibles for the two pins were sealed in Type 304 stainless steel capsules which were connected and positioned in a modified Mark-II loop such that the center of the test train was 2.54 cm (1 in.) below the centerline of the reactor. The modified Mark-II loop for the EOS-1 test had the upper and lower loop bends removed, as well as the sodium pump. A 0.762-mm (0.030-in.) thick tantalum epithermal filter extending 15.2 cm (6 in.) above and below the test train was installed to flatten the radial power profile to the pins.

The TREAT core loading for EOS-1 was identical to the F-1 loading, except that the hodoscope slot went south from the test section instead of north. Positioning and use of the instrumentation remained the same, as well as the numbering system for the control rods. However, the transient that was specified for EOS-1 was of a different type, and as a result the use of transient rods 1 and 2 was not the same as in F-1.

Original plans for the EOS-1 test called for a temperature-and-control-rod-limited exponential (peaked) burst with an initial step reactivity insertion of 4.7% $\Delta k/k$. This plan was abandoned in favor of a complete temperature-limited transient when it was found that delay times in the control system made consistent clipping of the rapid transient difficult. The new transient was initiated by driving the T-2 and T-1 transient rods out of the core while the outer ring of the SCRAM control rods (pairs #7, 8, and 10) were held inserted in the core about 7.6 cm (3 in.). The initial period of the power burst was 23 ms, and the duration of the burst was 100 ms. (measured as the full width at half-maximum). Core temperatures averaged greater than 800 K, as opposed to 500 K for the F-1 test transient.

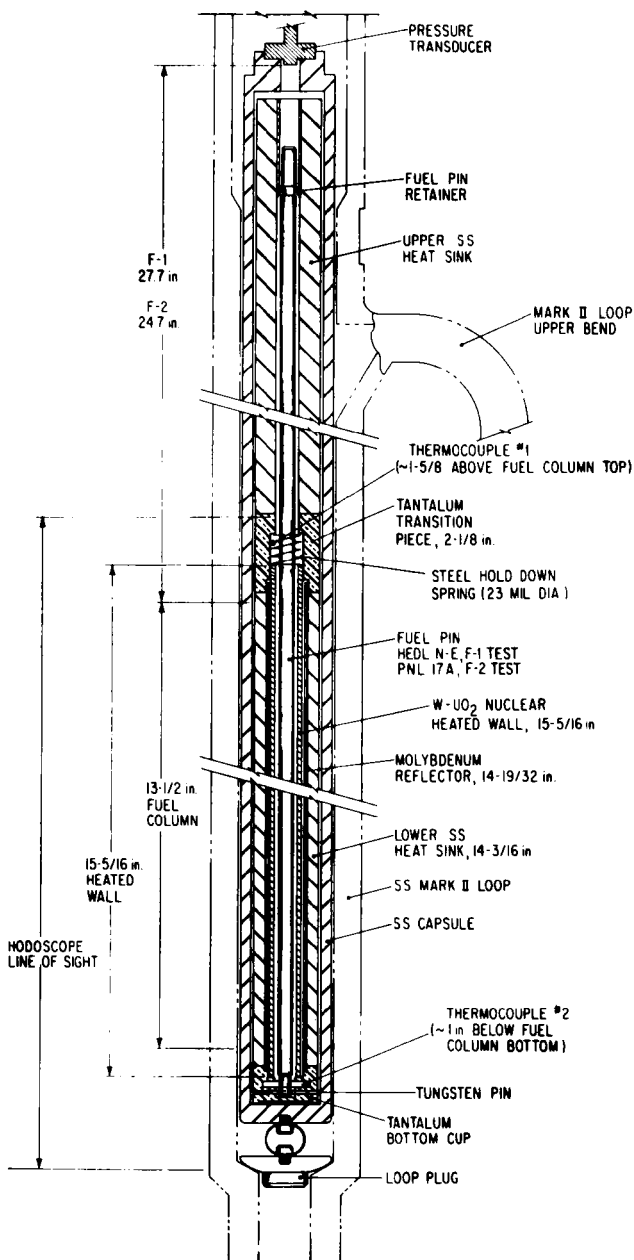


Fig. 6. Cutaway View of the EOS-1 Test Capsule (1 in. = 2.54 cm) (ANL Neg. No. 900-77-524).

III. POWER CALIBRATION TESTS FOR F-1 AND EOS-1

Before the actual F-1 and EOS-1 experiments involving fuel melting were performed, a series of transients and steady-state runs, called calibration tests, were made in TREAT. The main purposes of the tests were to determine the proper transients to be used for the F-1 and EOS-1 experiments and to determine the power calibration factors of the fuel pins for these transients. The technique employed was described in Section I as the transient-correction-factor (TCF) method. In this method, data obtained from monitor-wire irradiations are used to adjust the power calibrations for the fuel pins at low power to transient conditions. The calibration tests were also used for other purposes as described below.

One objective of the F-1 calibration test was to have the axial fuel-pin power shape match as nearly as possible the burnup shape of pins from EBR-II. Therefore, monitor wires were irradiated during the calibration test to determine the proper thickness for the dysprosium flux-shaping collars. In addition, the F-1 calibration test was used to analyze the neutron shadowing of power instruments by control rods.

The EOS-1 calibration test included reactor runs to determine the best thickness for the upper fuel-pin crucible, and to analyze the radiation and thermal effects of large, unshaped transients on the pressure transducers selected for the EOS-1 test. The calibration test was also used to continue the analysis of shadowing of detectors by the control rods. For this reason, different configurations of control rods from those normally used for steady-state runs were specified.

Before the results of the F-1 and EOS-1 calibration tests are given, two topics are discussed. The first concerns alternatives to the TCF method for determining the target pin power. The second deals with reactor runs performed prior to the F-1 test in which measurements were made of instrument shadowing during steady-state runs.

Alternatives to the TCF Method

All methods for determining the power calibration factor of the target pin have advantages and disadvantages associated with their use. Table 1, compiled by R. Simms for an experiment involving flowing sodium, lists the different techniques that can be used. Constraints such as the small number of fuel pins usually available for tests and the busy TREAT schedule result in the selection of the TCF method over other alternatives.

The last two alternatives mentioned in the table require a heat-balance calculation to determine the power in the target fuel. Coolant temperature and pressure data for the calculation are taken from the thermocouples and pressure transducers in the loop. However, these alternatives were not available for the F-1 and EOS-1 experiments, because the loop was removed and the target pins were dry-sealed in the test capsule.

Control-rod Shadowing of TREAT Instrumentation

A difficulty associated with the TCF method is that some uncertainty exists in determining the overall TREAT reactor power. In using the TCF

Table 1
 Alternatives to Determine Calibration
 Factors⁽⁵⁾

Approach	Pro	Con
1. Fresh fuel in mockup with planned transient. No sodium present (dry).	All factors nearly identical to test conditions.	Fuel would fail; loop and could not be analyzed easily. Safety is in question.
2. Fresh fuel in mockup loop with clipped transient (dry).	Conditions similar to an actual testing transient.	High risk of failing fuel unless factors known well enough.
3. Fresh fuel in mockup loop at low power level. Correct to transient using monitor-wire ratios - TCF (dry).	Low risk of fuel failure.	Approach may not be adequate to predict "transient correction."
4. Fresh fuel in loop at constant coolant flow (heat balance).	Test approaches actual test conditions.	No time available to commit loop. Sodium handling required (TREAT safety analysis report).
5. Irradiated fuel in loop at constant coolant flow (heat balance).	Test approaches actual test conditions; highly desirable.	Usually performed 1 day before test, and data, are not available for pre-test analysis.

method, this power must be determined for low-level and for trial transient runs. Further uncertainty is introduced because different instruments and control rods are normally used for low-level and transient runs. This was explained in the F-1 calibration report⁶ as follows:

"One of the inherent problems in attempting to conduct analytical experiments in TREAT is the necessity of using operational instrumentation as quantitative devices. The problem is compounded by the fact that different control rods affect the instrumentation in different ways depending on whether the control rod is near the sensor or on the other side of the core."

Prior to the F-1 calibration test, an attempt was made to determine the effect of different rods on TREAT detectors. Two low-power steady-state reactor runs were made at 80 kW, as measured by the linear power meter. The runs were performed with two different pairs of rods. The results are given in Table 2 (see Fig. 5 for the positions of the rods and detectors). The calibration values for the other instruments are based on the core power which was determined from a heat-balance calculation for the first run. A rod-pair position of 0 cm refers to rods that are completely inserted in the core.

Both the transient safety no. 1 and integrated power no. 1 sensors located at the northwest corner of the core showed a marked decrease in their calibration values when rod-pair no. 3 was used for steady-state run B. On the opposite side of the core, the control power channel and integrated power no. 2 sensor remained relatively the same.

Table 2

TREAT Instrument Calibrations
For Two Steady-state Runs⁷

	Run A	Run B
Rod #1 Position	88.09 cm (34.58 in.)	0 cm (0.0 in.)
Rod #3 Position	0 cm (0.0 in.)	72.09 cm (28.32 in.)
All other rods	Full out	Full out
Control Power Channel (SE)	1.03×10^{-7} A/MW	1.09×10^{-7} A/MW
Transient Safety #1 (NW)	0.166×10^{-7} A/MW	0.141×10^{-7} A/MW
Transient Safety #2 (SW)	0.225×10^{-7} A/MW	0.219×10^{-7} A/MW
Integrated Power #1 (NW)	0.071 ^{cv} /MW-s	0.059 ^{cv} /MW-s
Integrated Power #2 (SE)	0.81 ^{cv} /MW-s	0.079 ^{cv} /MW-s
Linear Meter (S-SW)	80 kW	80 kW
Calculated Power by Heat Balance	64 kW	Not determined

Results of F-1 Calibration Test

Because of the difficulty with the instrumentation, the calibration values from runs A and B above were averaged before being used to determine the reactor power during the F-series calibration runs. The calibration test served both the F-1 and F-2 experiments, because they had similar geometry and target fuel. The F-2 transient differed from the F-1 transient in that, after holding the 60 MW flat-top for about 6.5 s, the transient was ended in a power spike of over 700 MW.

The first run in the calibration test was a low-level, steady-state run lasting 3000 s with a fuel pin and a heated wall in the capsule. The power in the reactor was 50 kW as measured by the linear power meter. Following the run, the fuel pin was analyzed to determine the axial power profile and the low-level power calibration factor. The power in the fuel pin was obtained from radiochemical analysis by separating the fission product ^{140}Ba and ^{140}La and by measuring the buildup of lanthanum in the separated barium.⁷ The yield of ^{140}Ba from fission is known to great accuracy and can therefore be a measure of the total fissions which occurred in the sample.

The power calibration factor (PCF) was expressed in units of watts (generated at the axial peak power in the sample) per gram ^{235}U (in the sample) per MW (generated in the TREAT reactor). The value for the PCF for the fuel pin at low-level steady state was evaluated as follows:

$$\text{PCF}_{\text{LLSS}} = 2.56 \frac{\text{W (fuel pin)}}{\text{g } ^{235}\text{U (fuel pin)} \times \text{MW (TREAT)}}$$

A monitor wire of aluminum and uranium was also placed in the capsule in a hole parallel to the fuel-pin position in the stainless steel heat sink. The "power calibration factor" for the monitor wire for the low-level steady-state run was found to be

$$8.18 \frac{\text{W}}{\text{g } ^{235}\text{U} \times \text{MW}} .$$

Next, a low-level steady-state run was performed with the fuel pin and heated wall removed, and a new monitor wire placed in the heat sink. Control-rod pair no. 3 was used to control the run in the same manner as in the first low-power run. The difference in the power-meter readings was about 7%, a figure probably within the statistical variation of the meters and the reactor control system. The power calibration factor for this monitor-wire run was found to be

$$9.94 \frac{\text{W}}{\text{g } ^{235}\text{U} \times \text{MW}} ,$$

approximately 1.21 times larger than the previous value. The difference was

attributed to the increase in the thermal-neutron flux density when the fuel pin and heated wall were removed.⁶

Following the low-power runs, transients for F-1 and F-2 were performed in the reactor. Table 3 gives a summary of these transients. The computed TCF was determined by analyzing the monitor wires for their power calibration factors, and by dividing these values by

$$9.94 \frac{W}{g^{235}\text{U} \times \text{MW}},$$

the calibration factor for the low-level, steady-state, irradiated monitor wire. The TREAT integrated power used in the table was based on safety meter no. 1.

Several interesting results are indicated in the table. The most obvious is that the TCF was approximately the same for four different transients, including a clipped and an F-2 transient. Transient test no. 1593 was a clipped transient with the heated wall and fuel pin the test capsule (the monitor wire for the F-series was located in the stainless steel heat sink next to the heated wall). The monitor-wire power calibration for transient number 1593 decreased, producing a lower TCF of 1.15. If this value for the TCF is multiplied by 1.21 (the ratio of unfueled to fueled low-level monitor-wire calibrations), the result is 1.39. This seems to indicate that the lower TCF for transient no. 1593 represented the same proportional decrease in the neutron flux density because of the presence of the fuel and heated wall.

The most difficult value to explain is the TCF for transient no. 1570, an F-2 transient in which part of the flat-top was controlled by the T-2 control rods. It is possible that part of this large TCF is the result of control-rod shadowing of the instrumentation.

After the clipped transient no. 1593 was performed, the fuel pin was analyzed to determine the power calibration factor for comparison with the TCF-predicted calibration factor. The predicted value was 2.56×1.39 , or 3.56, whereas the actual value was 3.44, an error of about 3%. This result lends support to the TCF method.

Results of the EOS-1 Calibration Test⁹

TREAT instrumentation problems were avoided for the low-level steady-state runs for the EOS-1 calibration test by using the same control rods as for the peaked-burst EOS-1 transients. The transients were initiated by ejecting the T-1 and T-2 rods from the core, while the outer-ring rod-pairs 7, 8, and 10 remained in the core. As a result, the low-level, steady-state runs were performed using control-rod-pairs 7, 8, and 10, with all other rods withdrawn from the core.

The first set of runs in the calibration test was conducted with an upper BN crucible of 4.7 mm (185-mil)-thickness surrounding the test fuel pin. Another set was required when it was discovered that the upper fuel-pin power was too low because the TCF was found to be much lower than expected. Both

Table 3

Summary of Transients for the F-Series Calibration Test⁸

TREAT Transient No.	Total Integrated Reactor Power (MW-s)	Computed TCF	Time (s)	Integrated Power (MW-s)	Power (MW)	T2 Position (in.)	T1 Position (in.)	Comments
1569	750	1.39	0.0	0	0	18.7	4.3	F-1-like transient,
			4.28	26	66	18.3	11.2	Begin flat-top,
			14.3	737	78	21.4	37.6	End flat-top; scram.
1570	920	1.51	0.0	0	0	18.7	4.0	F-2-like transient,
			4.38	27	69	18.7	11.3	Begin flat-top; use T2.
			7.5	278	66	37.4	11.6	Switch to T1,
			11.7	573	70	37.3	21.6	Begin power spike,
			12.3	801	992	37.8	39.6	Peak power.
1589	138	1.39	0.0	0	0	17.2	4.0	Clipped transient,
			4.38	20	59	17.0	10.8	Begin flat-top,
			6.3	132	60	16.8	13.5	End flat-top.
1593	138	1.15	0.0	0	0	18.0	4.0	Clipped transient with fuel,
			4.62	26	59	18.0	11.2	Begin flat-top,
			6.45	132	59	18.0	14.4	End flat-top; scram.
1607	771	1.41	0.0	0	0	27.0	0.0	F-2-like transient,
			4.12	17	62	23.0	9.0	Begin flat-top,
			10.42	432	68	23.0	23.9	Begin power spike,
			11.14	669	711	23.0	40.6	Peak power,
			11.24	704	73	23.0	40.2	Scram,
			11.36	771	1	23.0	15.5	Peak integrated power.
1608	624	1.38	0.0	0	0	19.0	4.3	F-1-like transient,
			4.45	25	63	19.0	11.2	Begin flat-top
			13.4	610	68	19.0	32.1	End flat-top; scram.

the E-8 and F-series calibration tests reported a TCF value of about 1.40; however, the TCF for an EOS-1 transient with initial reactivity of 3.5% $\Delta k/k$ was equal to unity within experimental accuracy. For a transient with a larger reactivity insertion of 4.7% $\Delta k/k$, the TCF dropped even lower, to about 0.90, for the two fuel pins in the capsule.

Table 4 describes the first set of EOS-1 transients, which had the 4.7-mm-thick upper BN filter. Following these transients, runs were conducted with a new BN upper crucible of 2.29-mm (90-mil)-thickness. Unfortunately, the low-level, steady-state irradiation of a monitor wire in the thinner crucible was delayed because of routine TREAT maintenance. However, the results for the first set of transients are adequate for studying the transient correction factor.

Table 4

Summary of Selected EOS-1 Calibration Test Transients

TREAT Transient Number	Reactivity (% $\Delta k/k$)	Peak Power (MW)	Evaluated TCF		Position of Rods 7,8, and 10, cm with- drawn from core	Comments
			Upper Pin	Lower Pin		
1731	3.5	8,300	0.97	1.01	100.6 (7) 100.2 (8,10)	Clipped transient
1738	4.7	14,490	0.91	0.89	114.8	Clipped transient
1739	4.7	16,310	0.91	0.89	117.7	Clipped transient
1740	4.7	19,650	0.90	0.87	115.0	Clipped transient

IV. COMPUTER MODELING OF THE CALIBRATION TESTS

General Approach

Up until the present, the transient correction factor was used pragmatically in TREAT calibration tests to predict the fuel-pin power calibration factor, the validity of the method is questioned despite adequate success because of its unpredictable nature. A causal explanation of the TCF in terms of variables, such as test geometry, fuel type, and reactor transient control, is the objective of this study. Such an understanding is necessary for effective use of the TCF method.

As stated earlier, this study was conducted through computer simulation of the calibration tests using reactor-physics codes. The main code used was the one-dimensional radiation code ANISN which solves the Boltzmann transport equation by the discrete-ordinates method. A number of auxiliary computer programs were utilized to prepare the input cross-section data for ANISN (described in the next section). Advantages of this approach are the degree of control over important parameters as input and the detailed information available as output. An experimental program to explore the nature of the TCF method would involve considerable cost for the same flexibility.

However, the approach has a disadvantage which is shared by all modeling efforts, that is, simplifying assumptions must be made which will reduce the model complexity yet maintain the important factors of the modeled situation. Reactor temperatures, fuel-pin cross sections, reactor geometry, and control-rod positions during tests were the most important factors to be included in the reactor models. The following sections describe how they were handled in the modeling effort.

Cross Section¹⁰

For this study, a main library of neutron cross sections having 32 energy groups was generated using the AMPX code.* The library cross sections were written to be input in the ANISN format, which is relatively simple. In addition, computer codes have been written to change ANISN-formatted cross-section libraries into libraries that are utilized by other reactor-physics program.

The cross sections used had a P_1 -order approximation for anisotropic scattering. The energy-group structure contained 3 fast groups (10-0.11 MeV), 17 intermediate-groups (0.11 MeV-1.85 eV), and 12 thermal and epithermal groups (1.85 eV-0.0006 eV). Although only σ_{vf} , σ_a , σ_{total} , and the scattering cross sections are used in the ANISN calculation, the cross-section library for each material contained $(n,2n)$, (n,γ) , (n,α) , (n,p) , fission, and transport cross sections.

Cross sections evaluated at thermal-equilibrium temperatures of 300 to 900 K were developed for the TREAT core materials. Fuel-pin cross sections

* The code, its use in the study, and the 32-group ANISN library are described in Appendix C.

were generated at temperatures up to 2400 K. The uranium in the TREAT core was considered infinitely dilute in the graphite. A self-shielding calculation was performed in AMPX to correct the cross sections for the fissionable isotopes of the fuel pins for shadowing effects of one atom on another.

Other libraries generated during the study were a 199-group AMPX-formatted library, a 10-group ANISN library, and a 10-group library for use with the Argonne Reactor Code (ARC) system.¹¹

Reactor Modeling Using the ANISN Code

The anisotropic S_N code (ANISN) is a multigroup, one-dimensional discrete-ordinates transport code with anisotropic scattering.* The program was used to model the TREAT reactor with a single order of scattering (P_1) and 4 orders of angular quadrature (S_4). Neutron cross sections were provided by the 32-group ANISN-formatted library.

The TREAT reactor was represented in cylindrical geometry by 6 homogeneous zones outward from the edge of the experimental hole to the outer face of the reflector. Figure 7 illustrates the reactor zones. (Compare this diagram with the pseudocylindrical loading of the TREAT core in Fig. 5). The height of the core used in the computer calculation was 173.96 cm. (This is the active fuel height in the TREAT assemblies (121.92 cm) plus 52.04 cm for the TREAT extrapolated height).

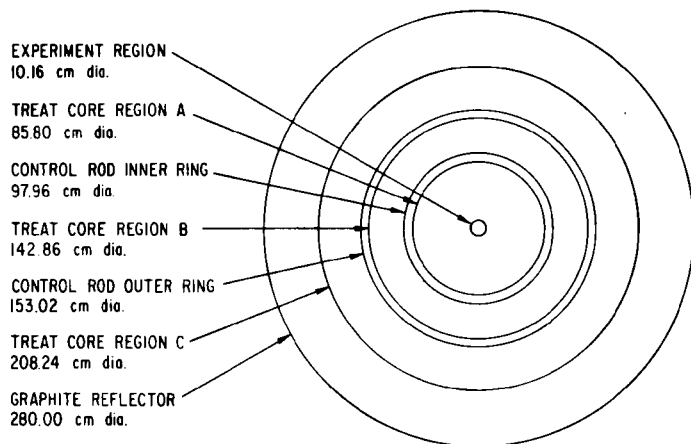


Fig. 7.

*ANISN Representation of
TREAT Core (ANL Neg. No.
900-77-523).*

The 5.1-cm (2-in.)-wide homogeneous control-rod rings were a mixture of TREAT core and control rod materials. The positions of the control rods in the core for each ring was simulated by changing the boron concentration of the rings. At first, the boron concentrations were determined directly from the number of control-rod boron atoms in the core. However, the reactor size had to be doubled for it to reach criticality. This is because the boron atoms that were spread around the ring were much more effective than the self-shielded atoms in the rods. As a result, the boron cross sections were altered to account for the dilution of boron atoms in the rings. The method used to reduce the boron cross sections is discussed in Appendix E.

*The ANISN code and the discrete-ordinate method for the solution of the Boltzmann transport equation are described in Appendix D.

Steady-state runs for the F-series calibration tests were modeled using 300 K for the TREAT core cross sections. The inner control-rod ring had a boron concentration of 1.421×10^{21} atoms/cm³ to represent rod pairs 1 and 3, which were used to control the low-level steady-state run. The outer-ring boron concentration was made very small because the outer rods were withdrawn from the core during these runs.

The EOS-1 steady-state runs also employed 300 K cross sections. However, the boron concentration in the inner control-rod ring was zero because these rods were withdrawn from the core. The outer ring had a boron concentration of 1.556×10^{21} atoms/cm³ to represent rod pairs 7, 8, and 10.

The F-1 transient was modeled using 500 K temperature cross sections for the core. Clipped F-1 transients were represented by using 400 K and 450 K cross sections. The outer-ring boron concentrations were determined from the position of the T-2 transient rods during the run. The inner-ring concentration was found by a concentration search on boron.

Two different F-2 transients were modeled. In the first, the outer-ring boron concentration was determined with the T-2 rods at a position of 58.4 cm (23 in.) as in transient number 1607. The second model had an outer-ring boron concentration corresponding to the T-2 rods at 95 cm (37.4 in.), their location during the power spike for the transient number 1570. Cross-section temperatures for both models were elevated to 700 K and the concentrations in the inner control-rod were determined by concentration searches with the system just critical.

For the F-series models, the fuel pin was represented as a separate region with an outer radius of 0.246 cm. Cross-section temperatures for the fissionable materials were set at 2100 K during transients and 300 K for steady-state runs. The fuel-pin cladding, the heated wall, and the molybdenum reflector were homogenized to form the second zone with an outer diameter of 1.194 cm. Cross-section temperatures were 900 K for transients and 300 K for steady-state runs. The final region for the experiment was made by homogenizing into a single zone the stainless steel capsule wall, heat sink, loop wall, and boron filter surrounding the loop. The outer diameter of the region was 10.16 cm, which extended to the inner face of the reactor core.

The EOS-1 calibration test transients were modeled using 700 K cross sections for the reactor core materials. The outer control-rod ring representing rod pairs 7, 8, and 10 had a concentration of 5.54×10^{20} atoms/cm³, which made the 700 K reactor just critical. Thus, the part of the transient being modeled was the peak of the power burst.

The two pins present in the EOS-1 test were handled separately in the computer models. Half of the EOS-1 models had the highly enriched upper pin in the center of the reactor, while the other used the lower pin. The outer diameter of the fuel-in region for both cases was 0.492 cm, which represented the fuel pins without their cladding. The next region surrounding the upper pins was a homogenized mixture of the cladding, boron nitride filter, and steel sleeve with an outer diameter of 1.906 cm. The lower pin had a region similar to this, but it had twice the amount of BN filter and no stainless steel sleeve. The final region for both cases had an inner diameter of 1.905 cm and an outer diameter of 10.16 cm extending to the reactor core. The

region was a homogeneous mixture of stainless steel from the capsules and loop, tantalum from the eipithermal filter surrounding the loop, and air from the loop wall to the inner face of the reactor. The cross-section temperature for the upper fuel pin was taken to be 2400 K during transient runs. For the lower pin 1800 K cross sections were used to represent transient temperatures.

Monitor-wire irradiations for the F-series calibration tests were simulated by replacing the fuel-pin region by a smaller one (of 0.08-cm outer diameter) representing the monitor wire. The cross-section temperature for the wire materials was 500 K for transients and 300 K for low-level steady-state runs. The heated wall and fuel-pin-cladding region were removed, and a smeared mixture of stainless steel and air extended from the wire to the first region of the core. For the EOS-1 tests, the fuel-in regions were replaced by a smaller monitor-wire region, and the gap which resulted was filled by enlarging the boron nitride filter region and by reducing its density.

V. RESULTS

Interpreting ANISN Output¹²

As a consequence of the computational methods of ANISN and the normalization of its output, the results for the power calibration coefficients are expressed below in slightly different units than previously defined.

By proper selection of options the user may have the ANISN code normalize all output to 1.0 fission neutron in the system per second or the user may supply a different value. If no value is specified, the output is normalized to a number selected by the code (this option is usually avoided because the code-selected number is not listed in the output). This normalization function of ANISN is acceptable because it does not change the ratio of power in the target to the TREAT power (i.e., the power calibration factor). In the present investigation the value of 1.0 for the normalization was specified for ease in comparing results.

When cylindrical geometry is used in ANISN, the code performs the discrete-ordinates calculation on a disk mesh, using the reactor height and the buckling factor to account for transverse leakage. Neutron flux densities from this mesh are used to generate output for a 1-cm-thick disk located at the half-height of the cylindrical system.

The volume formed in the target region by the 1-cm disk lies on the centerline of the reactor and represents the section of the target where the peak fissions occur. The computer output for the target regions does not have to be adjusted because the power calibration factor is expressed in terms of the peak value for the target.

On the other hand, the computer output for the TREAT core regions should be adjusted to determine the total power for use in the power calibration factor. However, the ratio of the power in the 1-cm slice of core at the reactor centerline to the average reactor power is very difficult to determine. In order to avoid computing a new factor for adjusting the output to the total TREAT power for each test, a different power calibration factor is calculated. The new factor still relates a measure of the power in the fuel pin monitor wire to the power in the TREAT core. The units for the power calibration are fissions in the target region (peak value) per 1.0 fission neutron per second in the system divided by the sum of the fissions in the core regions per 1 fission neutron per second in the system:

$$PC = \frac{\text{normalized fissions (Target)}}{\text{normalized fissions (TREAT)}}$$

Computed F-1 Transient Correction Factors

The results of four computer runs are listed in Table 5. The first two runs were made to establish the power calibration factors for the fuel pin and monitor wire at low-level steady-state TREAT operation. The second two computer runs simulated the F-1 transient to determine the power calibrations at transient conditions. The computed transient correction factor with the monitor wires

is 1.39×10^{-6} divided by 1.02×10^{-6} , or 1.36. The computed TCF for the fuel pin is 1.39. These values are in excellent agreement with the experimental values determined during the calibration tests. The results are significant in that the TCF for this model cannot be attributed to control-rod shadowing of the power meters. In the computer runs, the power in the core is determined directly by summing the fissions in all the core regions.

Table 5 illustrates the fact that there is a transient correction factor for each location in the core - not only at the center of the reactor where the target is located. The core-wide TCF is the result of the different power profiles in the reactor. In the steady-state run the radial profile of the thermal-neutron flux density is relatively flat because the reactor is controlled by the inner-ring control rods. But the F-1 transient is conducted with the T-2 rods in the outer ring at a constant position while the T-1 rods are withdrawn from the core. The effect of these rods is to increase the relative thermal-neutron flux density in the center of the reactor. Therefore, the power calibration factor, which relates the power in the target to the reactor power, increases in going from low-level steady-state to transient conditions for F-1.

Table 5
Results of F1 ANISN Runs

	Run Number			
	1	2	3	4
Target	F-1 Fuel Pin	Monitor Wire	Monitor Wire	F-1 Fuel Pin
Reactor Operation	F-Series Low-Level Steady-State	F-Series Low-Level Steady-State	F-1 Transient	F-1 Transient
Normalized Fissions				
Target Zone	2.08×10^{-4}	4.22×10^{-7}	5.75×10^{-7}	2.88×10^{-4}
Core Region A	0.067	0.067	0.084	0.084
Control Ring 1	0.014	0.014	0.018	0.018
Core Region B	0.115	0.115	0.120	0.120
Control Ring 2	0.029	0.029	0.026	0.026
Core Region C	0.187	0.187	0.164	0.164
Total Core	0.414	0.413	0.413	0.413
Power Calibration	5.02×10^{-4}	1.02×10^{-6}	1.39×10^{-6}	6.97×10^{-4}

Computed EOS-1 Transient Correction Factors

The results of the eight computer runs simulating the EOS-1 calibration test are given in Table 6. Each of the four different targets was irradiated for EOS-1 low-level steady-state and transient conditions. Computer runs 5 through 8 were performed with a 2.29-mm (90-mil)-thick BN filter surrounding the targets. A 4.7-mm (1.85-mil)-thick filter was used for the remaining runs. A mockup of the upper EOS-1 fuel pin (test pin) was used as the target for runs 5 and 6. In runs 9 and 10 the lower EOS-1 fuel pin (control pin) was the target.

Dividing the transient power calibrations by the low-power calibrations for each target gives the following transient correction factors: upper test pin, 1.02; upper monitor wire, 0.98; lower control pin, 0.96; lower monitor wire, 0.98. These values compare favorably with the experimental values listed in Table 4. Again, the monitor-wire TC's are reasonable predictions (within a 4% error) for the transient correction factors for the fuel pins.

The results of the EOS-1 ANISN runs illustrate, as in the F-1 runs, that each region of the reactor has a 'transient correction factor' resulting from changes in the radial reactor power shapes between steady-state and transient runs. However, the EOS-1 core-wide transient correction factors are closer to 1.0 for the center and outer reactor regions than the F-1 values. This is because the same rods were used for both steady-state and transient runs to reduce the difficulty in determining TREAT power. As a result, the radial power shapes for EOS-1 are a closer match than for F-1.

Although Tables 5 and 6 illustrate the major effect that the control rods have on the target TCF, data from the tables demonstrate that there is another factor which influences the target TCF. The TCF value for core region A in the F-1 runs is 1.24, while the TCF for the F-1 targets increases to about 1.30. In the EOS-1 computer results, the TCF for core region A is 0.87. The transient correction factors for the EOS-1 targets should have been below 0.87 if tilting of the reactor power shape by the control rods was the only factor influencing the target TCF. Instead, the average TCF for the EOS-1 targets is 0.985. The increase in the target TCF over the inner reactor region TCF in the EOS-1 and F-1 runs was 1.13 and 1.12, respectively.

As part of the investigation into the nature of this increase an F-1 type computer run was made. The experimental regions for this run contained the F-1 fuel pin, heated wall, and steel loop at transient temperatures. However, the reactor core temperatures and control-rod ring concentrations were kept for the F-1 low-level steady-state run. The fuel pin for this modified case (Run 13, Table 7) had a 1.12 TCF compared to the fuel pin in the original F-1 low-level steady-state run with all cross-section temperatures at 300 K. Therefore, part of the transient correction factor can be attributed to the higher temperatures in the loop and target during transient conditions.

The increase in the TCF as a result of the higher temperatures in the experimental regions can be explained in two ways. First, the higher TCF could be caused by transient temperatures in the target, a Doppler effect. On the other hand, the higher TCF could be attributed to transient temperatures in the steel structure surrounding the target. In order to test these two theories separately, two more modified F-1 low-level steady-state computer

Table 6
Results of EOS-1 ANISN Runs

	Run Number							
	5	6	7	8	9	10	11	12
Target	Upper Test Pin	Upper Test Pin	Upper Monitor Wire	Upper Monitor Wire	Lower Control Pin	Lower Control Pin	Lower Monitor Wire	Lower Monitor Wire
Reactor Operation	Low Level Steady-State	Transient	Low Level Steady-State	Transient	Low Level Steady-State	Transient	Low Level Steady-State	Transient
Normalized Fissions								
Target Zone	1.54×10^{-4}	1.57×10^{-4}	2.55×10^{-7}	2.50×10^{-7}	3.32×10^{-5}	3.19×10^{-5}	5.51×10^{-8}	5.44×10^{-8}
Core Region A	0.115	0.102	0.115	0.101	0.114	0.101	0.114	0.101
Control Ring 1	0.023	0.021	0.023	0.021	0.023	0.021	0.023	0.021
Core Region B	0.122	0.123	0.122	0.123	0.122	0.123	0.122	0.123
Control Ring 2	0.119	0.022	0.019	0.023	0.012	0.023	0.019	0.023
Core Region C	0.133	0.144	0.134	0.146	0.134	0.145	0.134	0.146
Total Core	0.413	0.414	0.414	0.414	0.413	0.414	0.413	0.414
Power Calibration	3.73×10^{-4}	3.73×10^{-4}	6.16×10^{-7}	6.04×10^{-7}	8.04×10^{-5}	7.71×10^{-5}	1.33×10^{-7}	1.31×10^{-7}

runs were performed with monitor wires as the targets. In the first, the monitor wire had a transient temperature of 500 K, while the surrounding steel region had a temperature of 300 K. For the second run these temperatures were reversed. The result of these runs are shown in Table 7 under Runs 14 and 15. The data from the first run show that the temperature change of the monitor wire alone does not significantly affect the TCF. On the other hand, when the steel region, representing the capsule and loop walls, is raised to transient temperatures, the TCF for the monitor wire is 1.10 when compared to the original monitor-wire low-power run.

Table 7
Results of Modified F-1 ANISN Runs

	Run Number			
	13	14	15	16
Target	Fuel Pin at 2100 K Steel at 900 K	Monitor Wire at 500 K Steel at 300 K	Monitor Wire at 300 K Steel at 500 K	Monitor Wire at 500 K Steel at 300 K
Reactor Operation	Low Level	Low Level	Low Level	F-1 Transient
Normalized Fissions				
Target Zone	2.33×10^{-4}	4.23×10^{-7}	4.68×10^{-7}	5.37×10^{-7}
Core Region A	0.067	0.067	0.067	0.082
Control Ring 1	0.014	0.014	0.014	0.018
Core Region B	0.115	0.115	0.115	0.126
Control Ring 2	0.029	0.029	0.029	0.028
Core Region C	0.188	0.188	0.188	0.162
Total Core	0.414	0.414	0.414	0.414
Power Calibration	5.63×10^{-4}	1.02×10^{-6}	1.13×10^{-6}	1.29×10^{-6}

A final modified F-1 computer run was made to verify the effect of hot steel on the TCF. For this run (number 16), the cross-section temperatures were the same as in Run 3, the F-1 transient with a monitor-wire target. However, cold instead of transient temperatures were used for the steel region.

The monitor wire TCF for this case was 1.27, whereas the TCF for the core region was 1.22. (This 1.22 is the average TCF for the inner core region; the TCF approaches 1.27 towards the inner edge of the region). Therefore, these calculations show that the heating of the steel surrounding the target contributes positively to the target TCF.

Transient Correction Factors for Clipped and F-2 Transients

Transients are clipped by scrambling the control rods before the reactor is completely shutdown by the temperature coefficient. A clipped transient can also refer to a shaped transient which is ended early. Temperatures for clipped transients are lower than those for full transients, making it possible to irradiated fuel pins without having them fail.

The clipped transient (1589) for the F-1 calibration test produced a TCF of 1.39 for the monitor wire. Table 8, Run 17, gives the results for the ANISN simulation of this transient. A temperature of 400 K was used for all the materials in run 17. The computed TCF for the monitor wire is 1.34, an error of 4%. However, the computed value is closer to the previous computed TCF of 1.36 for the full F-1 transient. The results support the experimental findings that the TCF does not change significantly for clipped transients.

Table 8

ANISN Results for Clipped and F-2 Transients

	Run Number	
	17	18
Target	Monitor	F-1 Fuel Pin
Reactor Operation	Clipped F-1	T2 and T1 Controlled F-2 Transient
Normalized Fissions		
Target Zone	5.66×10^{-7}	3.59×10^{-4}
Core Region A	0.084	0.086
Control Ring 1	0.015	0.022
Core Region B	0.120	0.123
Control Ring 2	0.027	0.024
Core Region C	0.168	0.147
Total Core	0.414	0.412
Power Calibration	1.36×10^{-6}	8.71×10^{-4}

The calibration test for the F-series included two T-2 transient reactor runs. The first run, 1570, used both the T-1 and T-2 rods to produce the transient, but the second run, 1607, was formed by moving only the T-1 rods.

The monitor-wire-generated TCF for transient 1570 was 1.51, a 9% increase over the average F-1 transient correction factor of 1.39. For transient 1607 it was 1.41, a 1.4% increase.

Transient run number 1570 was simulated with ANISN by using the rod positions and material temperatures for the peak of the F-2 power spike at the end of the transient. The computed TCF for the fuel pin was 1.74, representing a 25% increase over F-1 TCF values. The reason for this large TCF is that the computer run models the reactor for the power spike. This part of the transient accounted for only 38% of the total integrated power. The rest of the integrated power was generated during the flattop portion of the transient, which was controlled by the T-2 rods. As these outer-ring rods are withdrawn, the TCF for the fuel pin should decrease because the transient reactor power shape begins to match the low-level power shape. The net result of the lower TCF for the flattop portion of the transient and the higher TCF for the power spike is a net increase in the transient correction factor.

VI. SUMMARY AND CONCLUSIONS

Summary

The calibration tests conducted for the EOS-1 and F-series experiments produced many different transient correction factors as indicated in Tables 3 and 4. ANISN computer models were used to duplicate the experiments and to determine the nature of the experimental results.

Analysis of the first set of computer runs, which modeled the F-1 transient runs numbers 1569 and 1608, showed that the control-rod positions are the primary factor in determining the TCF value. The computer results of the EOS-1 calibrations test verified this finding, but also indicated that there was a secondary factor influencing the TCF. This was attributed to heating of the experiment structure surrounding the target during the transient. From the computer runs it was determined that this heating effect increased the TCF by about 10%. For the F-1 test, the TCF resulting from control-rod positions was 1.24 (determined by comparing normalized fissions for the inner core region for low-power and transient conditions). Combining the control-rod effect with the heating effect gives a TCF of 1.36. The control-rod effect on the TCF for the EOS-1 calculation was 0.87. The heating in the experimental steel region raised the TCF by 10% to 0.96. The transient correction factor predicted by monitor-wire data was within 5% error of the computer-mockup fuel-pin TCF for all cases.

The lower value of the TCF for the F-1 clipped transient number 1593 was the result of the presence of the fuel pin inside the capsule with the monitor wire. This was explained by comparing the results of this run with a low-level steady-state run conducted with both a monitor wire and fuel pin in the capsule.

Finally, computer runs were made to determine the effect of clipping the transient. It was demonstrated, as in the experiments, that clipping the transient does not significantly change the TCF. This is because a similar rod configuration to the full transient is used. Also, some temperature increase occurs in the experimental section.

Conclusions

Both the monitor-wire target and the TREAT power instruments measure in some way the neutron flux density at their locations. The monitor wire, as it is used in the calibration tests, serves as a thermal-neutron-flux integrating meter by storing information (fission products) on the number of fissions occurring in the wire during the reactor run. The measurements made by the monitor wire and the detectors surrounding the core are affected by the different positions of the control rods for low level steady-state and transient runs. In addition, the heating of the steel around the wire during a transient increases the thermal-neutron flux density relative to low power at the monitor-wire location.

The TREAT instruments are used to indicate core-wide variables. Therefore, they must be carefully calibrated to remove the local flux-density changes

caused by the different control-rod positions during low-power and transient runs. However, data from the monitor wire are not adjusted between low-power and transient runs. This is because the local changes of the flux density at the reactor center are exactly the information desired.

It is the conclusion of this study that the target TCF is a real effect caused by the factors mentioned above. The uncertainty in the calibration of the TREAT instrumentation does not influence the ability of the monitor wires to predict the transient correction factors for the fuel pins. Poorly calibrated TREAT instruments will produce a wrong power calibration factor for the fuel pin, but they will not affect the TCF values as long as the following are observed:

1. The low-level steady-state runs for the monitor wire and fuel pin use the same rod configuration and motion. The TREAT power for both runs is determined by the same instrument.
2. The transient runs for the monitor wire and fuel pin use the same rod configuration and motion. The TREAT power for both runs is determined by the same instrument.

It is concluded that the monitor-wire transient-correction-factor method successfully predicts the change in the fuel-pin power calibration from low-level to transient conditions for the experiments in this study. These experiments were conducted with single fuel pins which were dry sealed in the test capsules.

Although computer runs were not made for test capsules having fuel-pin clusters, it is believed that the monitor-wire method may still produce the proper TCF value for a fuel-pin cluster of less than 19 pins, if the entire cluster can be replaced by a single monitor wire in the calibration runs. This would be the case, for instance, if the relative fuel-pin power distributions in the separate pins of the cluster were very nearly the same and could be modelled by one-fuel-pin low-level run. However, for large clusters using 19 or more fuel pins, heating effects in the cluster could produce a different TCF than the value predicted from the monitor wire. Further study is recommended for analyzing the applicability of the monitor-wire method for predicting the TCF for fuel-pin clusters.

It is also believed that the presence of the linear induction pump and flowing sodium during the transient should not have a significant effect on the monitor-wire method. However, this should also be the subject of further study.

Finally, it is noted that the ANISN code was an effective tool in computing the transient correction factors, but a poor one in determining the proper power calibration factors. On the other hand, the Monte Carlo code KENO has the opposite capabilities. KENO, because it is a 3-dimensional code, can model the target and near-core regions accurately enough to predict the target power calibration. However, a KENO model of the entire TREAT reactor to determine the transient correction factors would be prohibitively expensive. Combination of the results of ANISN and KENO appears to be a favorable method for predicting the data for future calibration tests. An alternative approach, which should be studied further, is to use a time-dependent, 3-dimensional

transport code (modified for the TREAT reactor, if necessary). Such a code would better describe the axial variation of the materials in the test train. It could also model the motion of the different control rods and, therefore, it could predict the TCF value for transients with complex rod movements. It could also predict the time dependency of the power in the test pins as a function of the instantaneous TREAT power and therefore may more accurately predict the exact time of the onset of fuel melting.

APPENDIX A¹

A Description of the TREAT Reactor Components

The standard TREAT fuel assembly is shown in Figure A-1. It has a square cross section with a side length of 10.06 cm (3.96 in.) and an active fuel section 1.2 m (4 ft) long. The cladding material is Zircaloy. The core fuel material is uranium-oxide-bearing graphite with 93.24% of the uranium being ²³⁵U. The concentrations of the significant elements in the reactor fuel is given in Table A-1. Located above and below the fissionable material is a graphite reflector section that is 61 cm (2 ft) long and canned in aluminum. A 6.35 mm (1/4-in.) ribbed zirconium spacer separates the fuel from the reflector region, protecting the aluminum from high temperatures.

Table A-1

Material Composition of TREAT Fuel⁽¹³⁾

	g/cm ³ of fuel	atoms/cm ³ of fuel
²³⁵ U	3.89×10^{-3}	8.685×10^{18}
²³⁸ U	2.488×10^{-4}	6.297×10^{17}
O	4.494×10^{-4}	1.862×10^{19}
C	1.720	8.623×10^{22}
¹⁰ B	2.292×10^{-6}	1.380×10^{17}
¹¹ B	1.082×10^{-5}	5.922×10^{17}
Fe	1.035×10^{-3}	1.116×10^{19}
TOTAL	1.725	8.827×10^{22}

Several special fuel assemblies have been constructed which accommodate the control rods, dummy fuel, and experimental access to the reactor fluxes. These fuel assemblies, illustrated in Figure A-2, are simple modifications of the standard fuel assembly. The central cavity of TREAT can hold a maximum of 361 of these assemblies in a 19 x 19 array.

A permanent radial reflector of graphite blocks is stacked 61 cm (2 ft) thick around the core. The height of this reflector is 2.34 m (7 ft 8 in.), that is, 10.2 cm (4 in.) shorter than the combined height of the reflector and fuel regions in the standard assembly.

Core support is maintained by a 2.54-cm (1-in.)-thick steel grid plate which in turn rests on a concrete ledge. Support in the center of the plate is provided by steel stubs that are used to guide the control rods from the

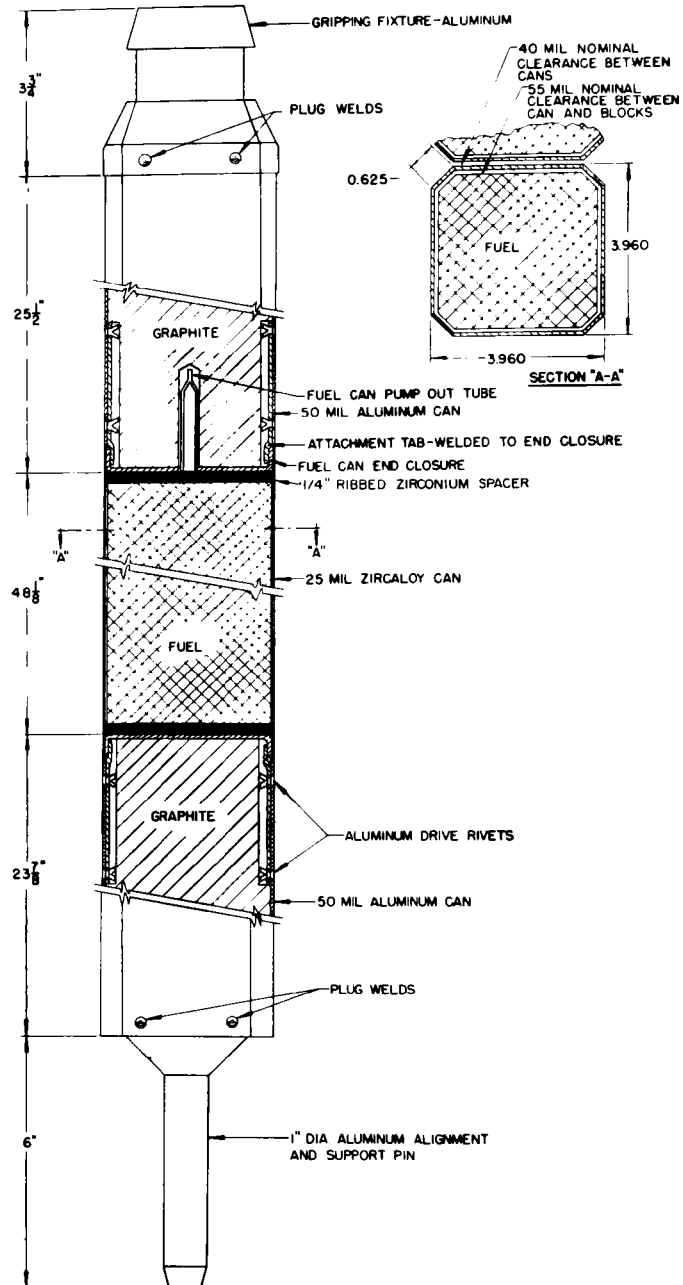


Fig. A-1. Standard TREAT Fuel Assembly
(ANL Neg. No. 900-77-502).

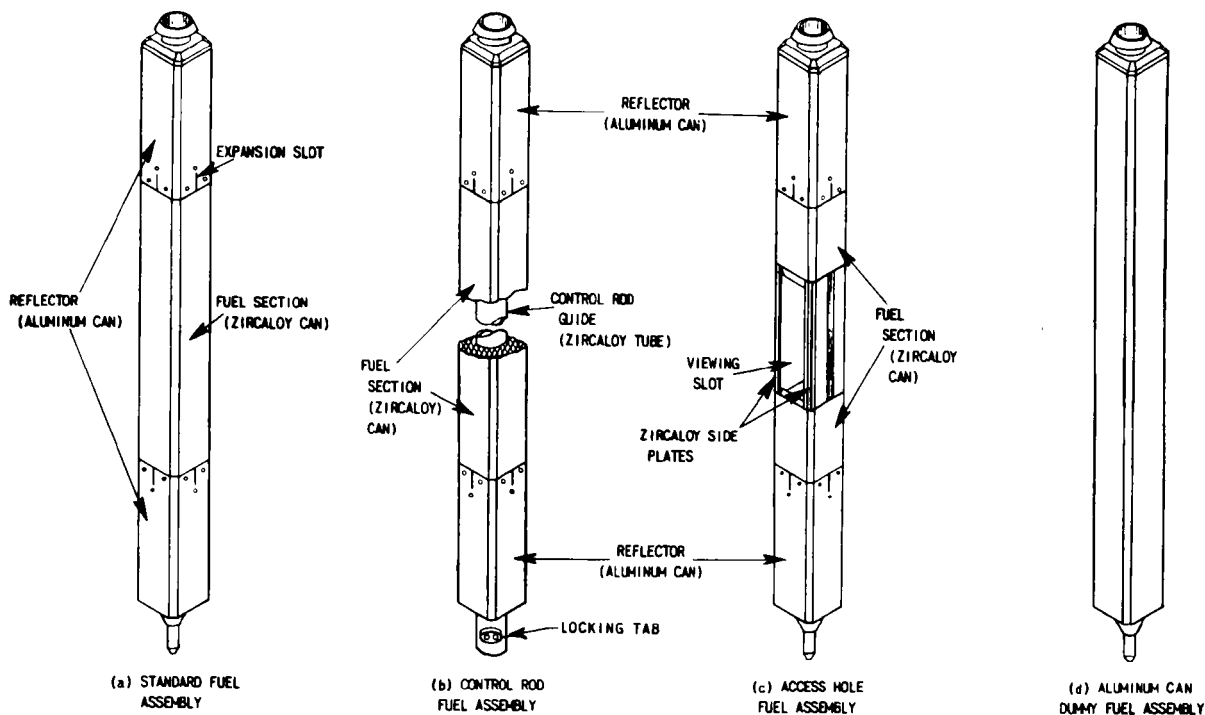


Fig. A-2. Types of TREAT Fuel Assemblies
(ANL Neg. No. 77-501).

lower reactor room. The grid has 32 possible control-rod-fuel-assembly locations. Depending on the core loading, special adapter plates are placed in control-rod fuel-assembly grid locations to accommodate standard or dummy fuel assemblies.

Each assembly has a device for alignment in the grid plate. The standard and dummy fuel assemblies have aluminum alignment pins which fit into the grid holes. They are centered in the tubes by 45° conical tapers on the top part of the pins. The control-rod fuel assemblies have hollow tubes which lock inside the steel guide tubes that support the grid plate. Locking is achieved by rotating the control-rod fuel assemblies 90° after they are placed in the core.

Four horizontal, calibrated rods, which extend from the shield, provide upper core support and rotational alignment. Each rod has a bar that pushes against an outer row of assemblies at the top of the core.

The TREAT control rods are 4.445 cm (1.75 in.) in diameter with 3.175-mm (1/8-in.)-thick walls. The poison section of each rod is composed of boron carbide (B_4C) powder compacted to a minimum density of 1.8 g/cm³. Carbon steel is the wall material for the poison section. The rods also have follower sections that are filled with graphite to reduce neutron streaming. For these sections Zircaloy is used as the wall material. The final two sections contain alternate layers of graphite and solid steel enclosed in a carbon-steel wall. The functions of these sections are to connect the main rod to the drive mechanisms, and to protect the drive mechanisms and lower reactor room from radiation.

Control rods are connected in pairs to drive mechanisms and are used as shut-down rods or transient rods. A transient rod is any control rod capable of adding reactivity at a rate greater than $0.0005 \Delta k/s$. The rate of reactivity addition is dependent upon the type of drive mechanism used for the rod pair and upon the position of the poison section of the rods relative to the graphite-filled section.

There are two types of control drives. The first uses an electric motor for slow-speed motion in the downward direction. These are not normally used to drive transient rods. The other is a hydraulic drive system capable of rod velocities as high as 4.138 m/s (170 in./s). High-performance servo valves are used with hydraulic drives to control the direction and velocity of rod motion.

Control-rod pairs connected to the motor-pneumatic drives are used for shut-down but can be converted to transient rods by changing the locations of the poison and graphite sections. In normal operation, boron carbide is located in the top section of the rod, which is pushed upwards out of the core. Thus, the pneumatic system can produce rapid shut-down. When the graphite section is at the top of the rod and the poison is the follower, use of the pneumatic system in the rod-up position will result in transient-rod reactivity additions.

Because of their high-speed capability, the two hydraulic drive mechanisms available at the site can produce transient-rod reactivity additions regardless of the positions of the poison and graphite sections. The active stroke of the hydraulic actuators is only 1.02 m (40 in.). For this reason the poison section of the rods that are connected to the hydraulic drives begins about 20 cm (8 in.) from the bottom of the core. Therefore, when the rods are ejected, all of their boron carbide is removed from the 122-cm (48-in.)-high core.

High-density concrete (215 lb/ft^3 or 3444 kg/m^3) with a thickness of 1.5 m (5 ft) is used as the reactor shield material outside the core and reflector to a height of 4.57 m (15 ft). Plates of 6.35-mm (1/4-in.) steel form the inner and outer jacket surfaces of the shield, although, the outside plate reaches a height of only 2.44 m (8 ft). Shielding above the reactor is composed of 0.91 m (3 ft) of removable concrete blocks. Beneath the concrete is a rotating shield-plug which has a penetration for changing fuel assemblies. The rotating shield-plug consists of three 10-cm (4-in.)-thick slabs of steel that are covered at the top and bottom of the plug by a 6.35-mm (1/4 in.) layer of boral. The bottom concrete shielding for TREAT (which also serves as the ceiling for the lower reactor room) is 0.91 m (3 ft) thick and is penetrated by control-rod guide tubes.

The east face of the reactor shield contains a 1.5-m (5 ft) square thermal column of graphite blocks which is shielded by a heavy concrete door, 83.8 cm (33 in.) thick. The three other faces of the reactor have penetrations through the side shield to permit viewing of the core. The center of the core and the experiments placed there are accessible through these penetrations when slotted fuel assemblies are used.

The reactor is cooled by air drawn through filters at the top of the shield. The air passes through the core within 1.588-cm (0.625-in.) square vertical coolant passages formed by the beveled edges of the fuel assemblies.

The faces of the concrete shield, permanent reflector, and core are separated by gaps which allow some cooling of the reflector. After leaving the core, the air is again filtered. Finally, two 29.84-kW (40-hp) turbo-compressor blowers are used to discharge the air through a stack to the atmosphere.

Remote control of the reactor is maintained from a building 760 m (2500 ft) away from the reactor building (3 manual SCRAM switches are located in the reactor building). Boron-10-coated ion chambers supply input to the control instrumentation. Located at the edges of the core, these detectors are connected to electronic circuits which measure reactor power and period during steady-state and transient operation of the reactor.

Circuits for measuring transient power and reactor period are also installed to supply input to the computer control system. The digital controller system can store a transient program, sense analog variables (reactor power period and hydraulic actuator positions) and convert them to digital form, and convert digital data to analog form for input to the transient-rod drives. This system gives the TREAT experimenter the capability to preprogram the reactor transient for accident simulation.

An instrument unique to the TREAT reactor is the fast-neutron hodoscope. The hodoscope has an array of fast-neutron detectors which determine fuel motion in the target pins as the test is being conducted. Fission neutrons from the target fuel pins stream through a row of slotted fuel elements to the edge of the reactor. They reach the detectors through a slotted block and are counted.

Some Reactor-physics Considerations

The minimum critical loading of TREAT was reached with 133 standard assemblies and 8 control-rod assemblies in a pseudo-cylindrical array containing 5.171 kg ^{235}U .

A typical experimental loading, on the other hand, requires a much larger core. A core having a test section in place of the central fuel assembly, two viewing slots, and an excess reactivity of 3.4% $\Delta k/k$, contains 244 standard, 16 slotted, and 16 control-rod assemblies. The control-rod assemblies are arranged to form two rings around the center.

The worth of an experiment replacing the central fuel element is about -3% $\Delta k/k$. For a typical experimental loading, the worth of a control-rod pair in the inner ring (46-cm radius) is about -4% $\Delta k/k$. It is about -2% $\Delta k/k$ for control-rod pairs in the second ring (74-cm radius).

There are two types of power bursts which are associated with the transients in the TREAT reactor: peaked and shaped bursts. The peaked bursts are initiated by step addition of reactivity and ended by a temperature-coefficient-induced shutdown. Control rods are sometimes used to clip the end of the transient after reactor power has been reduced by the negative temperature coefficient. Peaked bursts are the result of two separate physical effects in TREAT. The first is that the reactor has a large heat capacity and a minimal ability to cool during a transient. Secondly, the reactor has a negative temperature coefficient of about $-1.3 \times 10^3 \Delta k/k$ (referenced to peak temperature). It is negative because the increase in the average neutron temperature results

in higher neutron leakage. The maximum allowable core temperature of 600°C is reached by a peaked burst from a reactivity addition of 4.85% $\Delta k/k$. The maximum burst has a 21.8-ms period and produces a core-averaged, thermal-neutron fluence of about 7×10^{15} n/cm².

Shaped power bursts are usually controlled by the digital computer. The shape of the transients is derived from combinations of power flat-tops and peaked bursts. For a core containing 250 fuel assemblies the maximum integrated power is 1400 MW/s.

APPENDIX B

Descriptions of the F-1 and EOS-1 Fuel Pins
and Zr-U Monitor Wires

The F-1 fuel pin, described in Table B-1, was irradiated in the EBR-II reactor to a moderate burnup prior to the TREAT test. At mid-axis, the irradiated pin contained three microstructural zones and a central void.

For the EOS-1 experiment, two fuel pins placed axially in the core, one above the other, were tested simultaneously in the TREAT reactor. The fuel pins differed in uranium enrichment and outer diameter. The lower pin had a lower enrichment and a thicker cladding wall to prevent it from failing. Data for the upper pin and lower pin are described in Tables B-2 and B-3, respectively.

Characteristics of the monitor wires that were used during the F-1 and EOS-1 calibration tests to determine the transient correction factors are given in Table B-4.

Table B-1

F-1 Fuel-pin Data¹⁷

Type	HEDL N-E
Pin Number	N-077
Irradiated Peak Power	39.4 kw/m (12.0 kw/ft)
Irradiated Peak Burnup	2.35 a/o
Preirradiation Composition	75% UO ₂ -25% PuO ₂
U-235 Enrichment	77 a/o
Axial Length of Fuel Column	34.29 cm (13.5 in.)
Fuel Microstructural Dimensions (at Midaxis)	
Central-void Radius	0.41 mm (16 mils)
Columnar-region Radius	1.65 mm (65 mils)
Equiaxed-region Radius	1.73 mm (68 mils)
Unrestructured-region Radius	3.048 mm (120 mils)
Clad Dimensions (at Mixaxis)	
Inner Radius	2.500 mm (100 mils)
Outer Radius	2.921 mm (115 mils)
F-1 Plenum-gas Composition	99% Xe; 1% He
F-1 Plenum-gas Pressure	0.1344 MPa (12.1 psig)

Table B-2

Description of EOS-1 Upper Test Pin⁴

Type	ANL-A-EW
Pin Number	E-6-X
Fuel	UO ₂ -PuO ₂
Fuel Composition, Pu/(Pu + U)	0.250 ± 0.009
Plutonium Enrichment	88.0 ± 0.5 wt% ²³⁹ Pu + ²⁴¹ Pu in Pu
Uranium Enrichment	65.0 ± 1.0 wt% ²³⁵ U in U 0.5 wt% max. ²³⁸ Pu in Pu 11.0 ± 1.0 wt% ²⁴⁰ Pu in Pu
Fuel-pellet Diameter	4.940 ± 0.038 mm (0.1945 ± 0.0015 in.)
Fuel-column Length	10.16 ± 0.15 cm (4.00 ± 0.06 in.)
Fuel-pellet Density	10.09 g/cm ³ (nominal)
Fuel Planar Smear Density	9.42 ± 0.27 g/cm ³ (85% ± 2% T.D.)
Fuel Weight	19.6 ± 0.9 g
BN Pellet Diameter	4.951 ± 0.049 cm (0.195 ± 0.002 in.)
BN Pellet Length	1.290 ± 0.038 cm (0.500 ± 0.015 in.)
Cladding Dimensions	5.360 ± 0.025 mm (0.211 ± 0.001 in.) OD 1.27 ± 0.03 mm (0.005 ± 0.001 in.) wall 11.112 ± 0.041 cm (4.375 ± 0.016 in.) length
Gas Plenum Volume	0.115 cm ³ (nominal)
Plenum Gas	Helium
Gas Pressure (Room Temperature)	0.1 MPa (1.0 atm)

Table B-3

Description of EOS-1 Lower Control Pin

Type	ANL-A-EW
Pin Number	E-N-X
Fuel	UO ₂ -PuO ₂
Fuel Composition, Pu/(Pu + U)	0.250 ± 0009
Uranium Enrichment	Natural
Plutonium Enrichment	88.0 ± 0.5% wt ²³⁹ Pu + ²⁴¹ Pu in Pu 0.5 wt% max ²³⁸ Pu in Pu 11.0 ± 1.0 wt% ²⁴⁰ Pu in Pu
Fuel-Pellet Diameter	4.940 ± 0.038 mm (0.1945 ± 0.0015 in.)
Fuel-column Length	10.16 ± 0.15 cm (4.00 ± 0.06 in.)
Fuel-pellet Density	10.09 g/cm ³ (nominal)
Fuel Planar Smear Density	9.42 ± 0.27 g/cm ³ (95% ± 2% T.D.)
Fuel Weight	19.6 ± 0.9 g
BN Pellet Diameter	4.951 ± 0.049 mm (0.195 ± 0.002 in.)
BN Pellet Length	1.270 ± 0.038 mm (0.500 ± 0.015 in.)
Cladding Dimensions	5.842 ± 0.013 mm (0.2300 ± 0.0005 in.) OD 0.762 ± 0.025 mm (0.030 ± 0.001-in.) wall 11.112 ± 0.041 mm (4.375 ± 0.016 in.) length
Gas Plenum Volume	0.155 cm ³ (nominal)
Plenum Gas	Helium
Gas Pressure (Room Temp)	0.1 MPa (1.0 atm)

Table B-4

Description of Zr-U Monitor Wires

Composition, U/U+Zr	3.6 wt%
U-235 Enrichment	93.12%
Wire Diameter	0.81 ± 0.01 mm (31 ± 1 mils)
Wire Weight	30.51 mg/cm (77.5 mg/in.)
U-235 Weight	1.02 mg/cm (2.59 mg/in.)

APPENDIX C

The AMPX System and Generation
of Neutron-cross-section Data Set¹⁰

AMPX is a modular FORTRAN code which produces multigroup neutron, gamma-ray, and coupled neutron-gamma-ray cross-section data sets from ENDF/B libraries. The code was developed at the Neutron Physics Division of Oak Ridge National Laboratory (ORNL) and is available from the Reactor Shielding Information Center of ORNL.

There are 30 modules presently in the AMPX system, and any path through the modules is possible as long as the input requirements for each module are satisfied. Typically, a module performs calculations on a cross-section library and produces a new library as an output. Figure C-1 shows some possible paths between the major AMPX modules. The diagram illustrates that the cross-section libraries serve as an information link between modules. Included in the diagram is a dotted path showing the route taken through the AMPX system for this study.

The cross sections stored in the ENDF/B library are very general so as to permit their use in modeling a wide variety of nuclear processes. This generality is not required by most reactor codes. It is the function of the XLACS module to reduce this complexity by producing a weighted multigroup neutron-cross-section library. The cross sections in the XLACS-generated library can have a user-specified energy structure covering the full range of ENDF/B neutron energies. In addition, the order of expansion for the thermal scattering matrices and the scattering matrices above thermal can be specified by the user. Temperatures for evaluating the thermal scattering kernels can also be supplied as input.

XLACS was used in the study to generate a 119-group master neutron fine-group library. The number of thermal groups in this library was 30. A first-order expansion was made for the scattering matrices above thermal. Thermal scattering was assumed to be isotopic. Unresolved and resolved resonance calculations were performed at specified temperatures for all resonance nuclides. Thermal-scattering calculations were performed at 300 K for nuclides present in low-level steady-state reactor runs. Higher temperatures were specified for nuclides in transients.

The purposes of the Nordheim's Integral Treatment And Working Library (NITAWL) module are to perform resonance self-shielding calculations for the resonance nuclides and to reduce the generality in the master library. The Nordheim Integral Treatment is the usual method employed to perform the neutron-resonance self-shielding calculation. However, the narrow-resonance and infinite-mass treatments are available in the code. The cross-section library generated by NITAWL is called a working library.

The NITAWL module was used in the study to perform neutron-resonance self-shielding calculations using the Nordheim method for the fuel-pin resonance nuclides. Homogeneous geometry was used for all the self-shielding calculations, and the temperatures were varied over the range of fuel-pin temperatures. Each nuclide using the Nordheim Treatment requires as input, among other

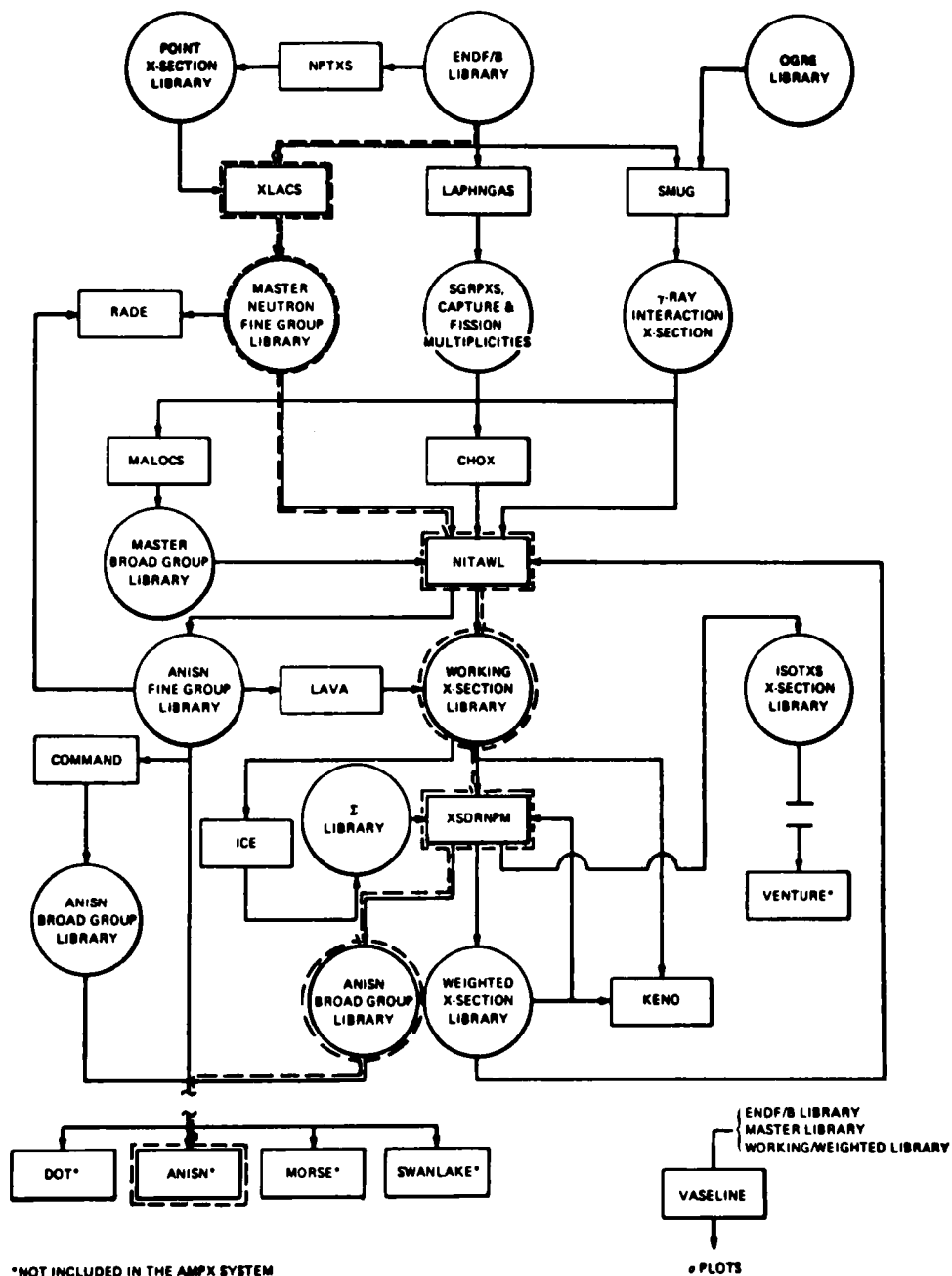


Fig. C-1. Possible Paths Between the Major AMPX Moduels (ANL Neg. No. 900-77-525).

parameters, the effective moderator scattering cross section σ_m , where

$$\sigma_m = \frac{N_m}{N_a} \sigma_s,$$

N_m is the moderator atom density (oxygen), N_a is the resonance-nuclide atom density, and σ_s is the moderator scattering cross section. All other nuclides were placed in the working library by NITAWL without a self-shielding calculation being performed.

The XSDRNPM module was used to collapse the 119-group working library to 32 groups and to convert the broad-group library to ANISN format. A one-dimensional, discrete-ordinates transport code is built into XSDRNPM for calculating neutron flux densities for spatial cross-section weighting.

For this investigation the 119-group (fine group) cross sections were collapsed using the TREAT-core flux spectrum. This spectrum was generated by a homogeneous volume of the TREAT core. The resulting 32-group ANISN-formatted neutron-cross-section library was stored on tape.

APPENDIX D

The Discrete-ordinates Method and the ANISN Code¹⁴

The discrete-ordinates (S_N) method provides for a numerical solution to the Boltzmann transport equation. The discrete-ordinates equation, which is derived from a conservative form of the Boltzmann transport equation, is a finite-difference equation in space, angle, and energy. As the space, angle, and energy mesh approaches differential size, the solution of the S_N equation apparently approaches the exact solution of the Boltzmann transport equation.

The derivation of the discrete-ordinates equation from the transport equation is contained in several sources, ¹⁴⁻¹⁶ and will not be detailed here. Basically the following steps are involved:

1. The phase space of the system is divided by a finite radius, angle, and energy mesh. Integrating over the intervals of the radius, angle, and energy mesh produces a set of finite-difference cells.
2. An integral operator, which implies a definite integral over the radius, angle, and energy of a finite difference cell, is applied to each term of the Boltzmann transport equation.
3. The integral over the energy interval is represented by the group angular flux density. The integrals over the angle and space intervals are evaluated using the mean-value theorem. In the process, the differential scattering cross section in the in-scattering term is approximated by a truncated Legendre polynomial expansion in the cosine of the scattering angle.

The resulting difference equation contains discrete flux-density variables that must be determined from cell boundary conditions and average values at the interval centers. Consequently, there are more unknowns than there are determining relations. The diamond difference technique solves this problem by relating the center and end-point flux densities in a consistent way.

ANISN solves the discrete-ordinates equations by performing a sweep of the mesh points. The code begins each sequence through the discrete points with the highest energy and proceeds to the lowest energy group. The angular sweep begins with the angular cosine of 1.0 and proceeds through the positive angular cosines in decreasing order. The spatial sequence begins at the boundary where inwardly directed flux values are specified, and the sweep is made to the other boundary. For negative angular cosines, the sweep starts at the opposite boundary, where reentering fluxes are usually zero, and proceeds to the source boundary.

A nested pair of iterative loops are required to produce a converged solution to the discrete-ordinates equation. In ANISN, an inner iteration for each energy group is performed for all directions and space cells. Each iteration computes a within-group scattering term which is based, in part, on data from the previous iteration. When the within-group scattering for two successive iterations differ by less than a predetermined criterion, the inner iteration is terminated. The calculation then proceeds to the next lower energy group.

The completion of all inner iterations for all energy groups is an outer iteration. During the outer iterations, the downscattering, upscattering, and fission sources are computed. The ANISN calculation is completed when these sources differ by a prescribed amount for two successive outer iterations.

APPENDIX E

Boron Cross Sections for Control Rods

The ANISN computer code permits only a one-dimensional description of the TREAT reactor. In cylindrical geometry, the various reactor zones are modeled as rings which surround the central target (the target represents a prototype fuel pin or a monitor wire). The TREAT control rods are difficult to represent in such a model. For simplicity, the boron control rods were homogenized with TREAT core material to form two rings. The thicknesses of the rings were chosen as the outer diameter of the original rods, i.e., 5.1 cm (2 in.).

The boron concentration of the control rods had to be adjusted for dilution by the fuel in the ring regions. In the solid control rods, the concentration of boron atoms is so great that the interior atoms are shielded from the thermal-neutron flux. The effective capture cross sections for the interior atoms is much lower than the infinitely dilute boron capture cross sections represented by ENDF/B data.

Therefore, the control-rod boron cross sections were adjusted to permit criticality of the TREAT mockup with an outer reactor radius about the same as the outer radius in the actual experiments. The adjusting factors for each energy group was determined from an ANISN run which made a search on boron concentration. The run, which used cylindrical geometry, had a center zone consisting of a smeared control rod. The second zone contained the homogenized reactor core materials. The volume of this zone was one-eighth of the reactor core volume included in the control-rod ring.

For each group the total fluxes for the control-rod zone were divided by the total fluxes for the surrounding core region. These ratios formed the adjusting factors, which were multiplied with the boron cross sections. Table E-1 give the original boron capture cross sections, the cross-section adjusting factor, and the new boron capture cross section for each group.

Without the adjustment, the TREAT reactor was critical with a radius of about 240 cm. Once the adjustment to the cross sections was made, the reactor became critical at 104.12 cm with the control rods set in the F-1 pretest position. In comparison, the reactor experimental outer radius formed by the pseudocylindrical array of fuel assemblies was 98.5 cm.

Table E-1

Changes to Boron Capture Cross Sections by Group

Group Number	σ_c for Natural Boron (barns) ^a	Adjusting Factor	New σ_c Boron (barns)
1	0.094	1.24	0.177
2	0.078	1.43	0.112
3	0.250	1.54	0.386
4	0.753	1.52	0.150
5	1.382	1.39	1.927
6	2.117	1.21	2.580
7	3.022	1.07	3.236
8	3.880	0.93	3.620
9	4.98	0.800	3.98
10	6.39	0.700	4.28
11	8.21	0.549	4.51
12	10.55	0.443	4.67
13	13.54	0.354	4.79
14	17.39	0.278	4.84
15	22.33	0.218	4.87
16	28.67	0.169	4.85
17	36.8	0.1315	4.84
18	47.2	0.1025	4.84
19	60.7	0.0795	4.83
20	80.0	0.0603	4.83
21	92.0	0.0518	4.77
22	100.6	0.0460	4.63
23	113.0	0.0417	4.72
24	128.4	0.0368	4.73
25	149.2	0.0317	4.73
26	180.6	0.0261	4.73
27	220.1	0.0214	4.72
28	264.9	0.0178	4.72
29	316.4	0.0149	4.72
30	403.3	0.0116	4.70
31	558.2	0.0083	4.68
32	945.1	0.0048	4.62

^a 1b = 10^{-28} m² 10^{-24} cm²

ACKNOWLEDGMENTS

The author would like to thank the many people who provided support during the execution of this study.

He is grateful to Dr. Herbert E. Hungerford and graduate committee members Phil Kier, and Professors Owen Gailar and Tom Palfrey for their constructive advice and guidance.

The author also acknowledges the assistance provided by Charles Dickerman, Bob Palm, Joe Tylka, Terry Lucitt, Bob Boyar, Orlo McNary, and Bill Knapp of Argonne National Laboratory.

This work was performed under ANL contract No. 109-38-3313 with Purdue University.

REFERENCES

1. Description of TREAT Facility, Unpublished Revision of Section III of Hazards Summary Report on the Transient Reactor Test Facility (TREAT), ANL-5923 (Sept 1971).
2. R. G. Palm, S.M. Gehl, C. L. Fink, R. R. Stewart, A. B. Rothman, and A. De Volpi, F-2 Phenomenological Test on Fuel Motion, Trans. Am. Nuc. Soc., p. 354 (June 1976).
3. R. G. Palm, Argonne National Laboratory, private communication.
4. J. P. Tylka, Specification of Calibration Experiments for EOS-1/2 Tests, Argonne National Laboratory, private communication (Aug 1975).
5. R. Simms, Argonne National Laboratory, private communication.
6. C. C. McPheeters, Data from the F-Series Calibration Experiment, Argonne National Laboratory, private communication (June 24, 1974).
7. A. E. Wright, D. Stahl, G. S. Stanford, A. B. Rothman, C. E. Dickerman, and L. J. Harrison, Transient Overpower Test H5 on FFTF-Type 'Intermediate-Power' Fuel, ANL report, to be published.
8. R. G. Palm, private communication (Aug 1976).
9. J. P. Tylka, EOS-1 and EOS-2 Calibration Test Results and Calibration Factors, Argonne National Laboratory, private communication (Aug 1976).
10. N. M. Greene, J. L. Lucius, L. M. Petrie, W. E. Ford, III, J. E. White, and R. Q. Wright, AMPX: A Modular Code System for Generating Coupled Multigroup Neutron-Gamma Libraries from ENDF/B, ORNL/TM-3706 (Mar 1976).
11. L. C. Just, H. Henryson, II, A. S. Kennedy, S. D. Sparck, B. J. Toppel, and P. M. Walker, The System Aspects and Interface Data Sets of the Argonne Reactor Computation (ARC) System, (Apr 1971).
12. W. W. Engle, Jr., A User's Manual for ANISN, ORNL Report K-1693, (Mar 1967).
13. R. O. Brittan, Survey and Status of TREAT Coverter, Argonne National Laboratory, private communication, (Nov 1971).
14. N. M. Schaeffer, Reactor Shielding for Nuclear Engineers, U. S. Atomic Energy Commission, Oak Ridge, Tennessee, Ch. 4, (1973).
15. H. Greenspan, C. N. Kelber, and D. Okrent, Computational Methods in Reactor Physics, Gordon and Breach Science Publishers, New York, N.Y., Ch. 3 (1968).
16. J. A. Maniscalco, An Analytical Treatment of Photon Transport in Two-Layered Media, Ph.D. Thesis, Purdue University, W. Lafayette, Indiana (1973).

Distribution for ANL-78-31Internal:

J. A. Kyger	A. J. Goldman	A. E. Wright
R. Avery	D. Rose	J. Ulrich
L. Burris	I. Bornstein	R. E. Boyar
D. W. Cissel	D. R. Ferguson	O. McNary
S. A. Davis	L. Baker	M. Kurtz
B. R. T. Frost	P. A. Lottes	P. I. Parks (2)
D. C. Rardin	T. C. Chawla	R. E. Henry
R. J. Teunis	W. C. Lipinski	D. R. Pedersen
C. E. Till	R. A. Noland	J. H. Tessier
R. S. Zeno	A. E. Klickman	D. H. Lennox
C. E. Dickerman	L. W. Deitrich	P. Kier
H. K. Fauske	D. H. Cho	B. Knapp
S. Fistedis	B. A. Korelc (3)	G. Klotzkin
B. D. LaMar	D. L. Graff (10)	A. B. Krisciunas
J. F. Marchaterre	R. G. Palm	ANL Contract File
H. O. Monson	J. P. Tylka	TIS Files (6)
R. Sevy	R. Simms	ANL Libraries (5)
	A. B. Rothman	

External:

DOE-TIC, for distribution per UC-79p (282)
 Manager, Chicago Operations Office
 Chief, Chicago Patent Group
 Director, Reactor Programs Div., CH
 Director, CH-INEL
 Director, DOE-RRT (2)
 President, Argonne Universities Association
 Reactor Analysis and Safety Division Review Committee:
 S. Baron, Burns and Roe, Inc.
 W. Kerr, U. Michigan
 M. Levenson, Electric Power Research Inst.
 S. Levy, S. Levy, Inc.
 R. B. Nicholson, Exxon Nuclear Co., Inc.
 D. Okrent, Univ. California, Los Angeles
 N. C. Rasmussen, Massachusetts Inst. Technology

ARGONNE NATIONAL LAB WEST



3 4444 00010810 0